A population of adult satellite-like cells in Drosophila is maintained through a switch in RNA-isoforms

Hadi Boukhatmi, Sarah Bray

Title: A population of adult satellite-like cells in *Drosophila* is maintained through a switch in RNA-isoforms

Authors: Hadi Boukhatmi and Sarah Bray*

Department of Physiology Development and Neuroscience,
University of Cambridge
Downing Street
Cambridge, CB2 3DY, UK

*corresponding author: sjb32@cam.ac.uk

Summary

Adult stem cells are important for tissue maintenance and repair. One key question is how such cells are specified and then protected from differentiation for a prolonged period. Investigating the maintenance of *Drosophila* muscle progenitors (MPs) we demonstrate that it involves a switch in *zfh1/ZEB1* RNA-isoforms. Differentiation into functional muscles is accompanied by expression of *miR-8/miR-200*, which targets the major *zfh1-long* RNA isoform and decreases Zfh1 protein. Through activity of the Notch pathway, a subset of MPs produce an alternate *zfh1-short* isoform, which lacks the *miR-8* seed site. Zfh1 protein is thus maintained in these cells, enabling them to escape differentiation and persist as MPs in the adult. There, like mammalian satellite cells, they contribute to muscle homeostasis. Such preferential regulation of a specific RNA isoform, with differential sensitivity to miRs, is a powerful mechanism for maintaining a population of poised progenitors and may be of widespread significance.

INTRODUCTION

Growth and regeneration of adult tissues depends on stem cells, which remain undifferentiated while retaining the potential to generate differentiated progeny. For example, muscle satellite cells (SCs) are a self-renewing population that provides the myogenic cells responsible for postnatal muscle growth and muscle repair (Chang and Rudnicki, 2014). One key question is how tissue specific stem cells, such as satellite cells, are able to escape from differentiation and remain undifferentiated during development, to retain their stem cell programme though-out the lifetime of the animal.

It has been argued that the progenitors of *Drosophila* adult muscles share similarities with satellite cells and thus provide a valuable model to investigate mechanisms that maintain stem cell capabilities (Aradhya, et al., 2015; Figeac, et al., 2007). After their specification during embryogenesis, these muscle progenitors (MPs) remain undifferentiated throughout larval life before differentiating during pupal stages. For example, one population of MPs is associated with the wing imaginal disc, which acts as a transient niche, and will ultimately contribute to the adult flight muscles. These MPs initially divide symmetrically to amplify the population. They then enter an asymmetric division mode in which they self-renew and generate large numbers of myoblasts that go on to form the adult muscles (Gunage, et al., 2014). In common with vertebrates, activity of Notch pathway is important to maintain the MPs in an undifferentiated state (Gunage, et al., 2014; Mourikis and Tajbakhsh, 2014; Mourikis, et al., 2012; Bernard, et al., 2010). To subsequently trigger the muscle differentiation program, levels of Myocyte Enhancer factor 2 (Mef2) are increased and Notch signalling is terminated (Elgar, et al., 2008; Bernard, et al., 2006). Until now it was thought that all MPs followed the same fate, differentiating into functional muscles. However, it now appears that a subset persist into adulthood forming a population satellite-like cells ((Chaturvedi, et al., 2017) and see below)). This implies a mechanism that enables these cells to escape from differentiation, so that they retain their progenitor-cell properties.

The *Drosophila* homologue of ZEB1/ZEB2, ZFH1 (zinc-finger homeodoman 1), is a candidate for regulating the MPs because this family of transcription factors is known to repress Mef2, to counteract the myogenic program (Siles, et al., 2013; Postigo, et al., 1999). Furthermore, *zfh1* is expressed in the MPs when they are specified in the embryo and was shown to be up-regulated by Notch activity in an MP-like cell line (DmD8) (Figeac, et al., 2010; Krejci, et al., 2009). In addition, an important regulatory link has been

established whereby microRNAs (miRs) are responsible for down-regulating ZEB/Zfh1 protein expression to promote differentiation or prevent metastasis in certain contexts (Zaravinos, 2015; Vandewalle, et al., 2009). For example, the miR-200 family is significantly up-regulated during type II cell differentiation in fetal lungs, where it antagonizes ZEB1 (Benlhabib, et al., 2015). Likewise, *miR-8*, a *miR-200* relative, promotes timely terminal differentiation in progeny of Drosophila intestinal stem cells by antagonizing *zfh1* and escargot (Antonello, et al., 2015). Conversely, down-regulation of *miR-200* drives epithelial mesenchymal transition (EMT) to promote metastasis in multiple epithelial derived tumours (Korpal, et al., 2008; Park, et al., 2008). Such observations have led to the proposal that the ZEB/miR-200 regulatory loop may be important in the maintenance of stemness, although examples are primarily limited to cancer contexts and others argue that the primary role is in regulating EMT (Antonello, et al., 2015; Brabletz and Brabletz, 2010). The MPs are thus an interesting system to investigate whether this regulatory loop is a gatekeeper for the stem cell commitment to differentiation.

To investigate the concept that ZEB1/Zfh1 could be important in sustaining progenitor-type status, we examined the role and regulation of *zfh1* in *Drosophila* MPs/SCs. Our results show that *zfh1* plays a central role in the maintenance of undifferentiated MPs and, importantly, that is expression is sustained in a population of progenitors that persist in adults (pMPs) through the activity of Notch. Specifically these pMPs express an alternate short RNA isoform of *zfh1* that cannot be targeted by *miR-8*. In contrast, the majority of larval precursors express a long isoform of *zfh1*, which is subject to regulation by *miR-8* so that Zfh-1 protein levels are suppressed to enable differentiation of myocytes. Expression of alternate *zfh1-short* isoform is thus a critical part of the regulatory switch to maintain a pool of progenitor “satellite-like” cells in the adult. This type of regulatory logic, utilizing RNA isoforms with differential sensitivity to miRs, may be of widespread relevance for adult stem cell maintenance in other tissues.

RESULTS

Zfh1 is required for maintenance of muscle progenitors

As zfh1 was previously shown to antagonize myogenesis (Siles, et al., 2013; Postigo, et al., 1999) it is a plausible candidate to maintain the muscle progenitor (MP) cells in *Drosophila* and prevent their differentiation. Its expression is consistent with this hypothesis as Zfh1 is present throughout the large group of MPs associated with the wing disc, which can be distinguished by the expression of Cut (Ct) (Figure 1A-A''). At early stages Zfh1 expression is uniform (Figure 1-figure supplement 1), but at later stages the levels become reduced in the cells with high Cut expression (Figure 1A''). These cells give rise to the direct flight muscles (DFMs), whereas the remaining MPs, where Zfh1 expression is high, give rise to the indirect flight muscles (IFMs) (Figure 1A''; (Sudarsan, et al., 2001)). Zfh1 expression in MPs is therefore regulated in a manner that correlates with different differentiation programs.

To determine whether Zfh1 is required in the MPs to antagonize myogenic differentiation we tested the consequences from silencing *zfh1* specifically in MPs, using *1151-Gal4* to drive expression of interfering RNAs (RNAi). Two independent RNAi lines led to the premature expression of Tropomyosin (Tm), a protein normally expressed in differentiated muscles, in the most severe (KK103205 line) ~80% of *zfh1*-depleted wing discs exhibited Tm expression (Figure 1B-C and Figure 1-figure supplement 1D-G). Similarly, expression of a Myosin Heavy Chain (MHC) reporter was detected in ~20% of *zfh1 (*KK103205*)* depleted wing discs (Figure 1-figure supplement 1H-I) indicating that small muscle fibers had formed precociously. Consistent with the premature expression of these muscle differentiation markers, decreased *zfh1* led to abnormal β-3Tubulin staining, showing that the residual cells had altered cell morphology in 90% of *zfh1*-depleted wing discs, (Figure 1B'-C'). These results demonstrate that reduced *zfh1* expression causes MPs to initiate the muscle differentiation program indicating that *zfh1* is required to prevent MP differentiation.

Lineage tracing experiments suggest that a subset of wing disc MPs have characteristics of muscle stem cells and remain undifferentiated even in adult *Drosophila*. Recently, these have been shown to express Zfh-1 (Chaturvedi, et al., 2017; Gunage, et al., 2014), which is compatible with our observation that Zfh-1 is necessary to prevent differentiation in MPs. In agreement, adult IFM muscle fibers were associated with sparse nuclei that retained

high levels of Zfh1 expression whereas the differentiated muscle nuclei exhibited no detectable expression (Figure 1D-D'). To better characterise these Zfh1 positive (+ve) adult cells, we expressed a membrane-tagged GFP (*UAS-Src::GFP*) under the control of a specific muscle driver *mef2-Gal4* (*mef2>GFP*). This confirmed that Zfh1 was expressed in myogenic *mef2>GFP*-expressing cells, and revealed that these cells were closely embedded in the muscle lamina (Figure 1E-E'''). Although many of the Zfh1 expressing cells were clearly co-expressing Mef2>GFP, Zfh1 was also detected in another population that lacked Mef2 expression. Often clustered, these cells were co-labelled with a plasmatocyte marker P1/Nimrod indicating that they are phagocytic immune cells (Figure 1-figure supplement 2). A subset of the Zfh1+ve cells are therefore myogenic and have characteristics of persistent muscle progenitors that likely correspond to the so-called adult satellite cells recently identified by others (Chaturvedi, et al., 2017) (Figure 1D-E).

The results demonstrate that Zfh1 is expressed in MPs, where it is required for their maintenance, and that its expression continues into adult-hood in a small subset of myogenic cells. If, as these data suggest, Zfh1 is important for sustaining a population of a persistent adult progenitors, there must be a mechanism that maintains Zfh1 expression in these cells while the remainder differentiate into functional flight muscles.

zfh1 **enhancers conferring expression in MPs**

To investigate whether the maintenance of Zfh1 expression in larval and adult MPs could be attributed to distinct enhancers, we screened *enhancer-Gal4* collections (Jenett, et al., 2012; Jory, et al., 2012; Manning, et al., 2012) to identify *zfh1* enhancers that were active in larval MPs. From the fifteen enhancers across the *zfh1* genomic locus that were tested, (Figure 2 and Figure 2-figure supplement 1 A) three directed GFP expression in the Cut expressing MPs at larval stages (Figure 2B-D). These all correlated with regions bound by the myogenic factor Twist in MP-related cells (Figure 2-figure supplement 1A; (Bernard, et al., 2010)). Enhancer 1 (Enh1; VT050105) conferred weak expression in scattered progenitors (Figure 2B). Enhancer 2 (Enh2; VT050115) was uniformly active in all MPs and also showed ectopic expression in some non-Cut expressing cells (Figure 2C). Finally, Enhancer 3 (Enh3; GMR35H09) conferred expression in several MPs with highest levels in a subset located in the posterior (Figure 2D). Enh3 encompasses a region that was previously shown to be bound by Su(H) in muscle progenitor related cells, hence may be regulated by Notch activity (Figure 2-figure supplement 1A; (Bernard, et al., 2010; Krejci,

et al., 2009). These results demonstrate that several enhancers contribute to *zfh1* expression in the MPs.

To determine which enhancer(s) are also capable of conferring *zfh-1* expression in adult pMPs we assessed their activity in adult muscle preparations. Only Enh3 exhibited any activity in these cells (Figure 2E), where it recapitulated well Zfh1 protein expression (Figure 2E-E''). Thus, Enh3-GFP was clearly detectable in scattered cells, which were closely apposed to the muscle fibers and contained low levels of Mef-2 (Figure 2E''), and was not expressed in differentiated muscle nuclei (Figure 2).

During pupal stages MPs migrate and surround a set of persistent larval muscles that act as scaffolds for the developing IFMs (Roy and VijayRaghavan, 1998; Fernandes, et al., 1991). By 18-22hr after puparium formation (APF), fusion of myoblasts is ongoing and by 30-36hr APF, most myoblasts have fused and myogenesis is advanced. By this stage, Zfh1 expression is already restricted to single cells (Chaturvedi, et al., 2017). We therefore examined Enh3 activity during the pupal period, using *Enh3-Gal4>UAS-GFP*, which yields a higher level of expression than the direct *Enh3-GFP* fusion. At 18-22hr APF, Enh3 activity was detected in both differentiating myoblasts (inside muscle templates) and undifferentiated MPs (between and around muscle templates) (Figure 2F'-F''). Importantly, a subset of MPs located between muscle templates exhibited higher levels of Enh3 expression and of Zfh1 levels (Figure 2F'), whereas lower levels were present in the differentiating myoblasts. By 30-36hr APF Enh3 expression was restricted to pMPs, which expressed high level of Zfh1 and were closely apposed to the muscle fibers (Figure 2G-G''). At the same stage, we consistently detected a small number of Zfh1+ve cells that lack detectable Enh3 expression and we speculate that these are undergoing differentiation, since myogenesis is still ongoing at this stage (Figure 2G). In general however, there is a strong correlation between Enh3 expression and the establishment of the adult Zfh1+ve pMPs, suggesting that Enh3 is responsible for maintaining *zfh1* transcription in this progenitor population during the transitionary phase between 20hr and 30hr APF.

If Enh3 is indeed responsible for expression of *zfh1* in MPs and pMPs, its removal should curtail *zfh1* expression in those cells. To test this, Enh3 was deleted by Crispr/Cas9 genome editing (∆Enh3; see material and methods). ∆Enh3 homozygous flies survived until early pupal stages allowing us to analyze the phenotype at larval stages. As predicted, ∆Enh3 MPs exhibited greatly reduced Zfh1 protein expression (Figure 2-figure supplement 1B-D) that correlated with decreased *zfh1* mRNA levels (Figure 2-figure supplement 1E). Although striking, the effects of ∆Enh3 did not phenocopy those of depleting *zfh1* using

RNAi, as no premature up-regulation of muscle differentiation markers (MHC, Tm) occurred in ΔEnh3 discs (data not shown). This is likely due to residual *zfh1* mRNA/protein (Figure 2-figure supplement 1), brought about by the activity of other *zfh1* enhancers (e.g. Enh1 and Enh2, Figure 2B-C). Nevertheless, it is evident that Enh3 has a key role in directing *zfh1* expression in MPs/pMPs.

Adult Zfh1+ve MP cells contribute to flight muscles

By recapitulating Zfh1 in adult MPs, Enh3 provides a powerful tool to investigate whether the persistent MPs are analogous to muscle satellite cells, which are able to divide and produce committed post-mitotic myogenic cells that participate in muscle growth and regeneration. To address this we used a genetic G-trace method, which involves two UAS reporters, an RFP reporter that directly monitors the current activity of the Gal4 and a GFP reporter that records the history of its expression to reveal the lineage (Evans, et al., 2009). When *Enh3-Gal4* was combined with the G-trace cassette RFP expression was present in the muscle-associated pMPs, which have low Mef2 expression (Figure 3A-A''). Strikingly, most of the muscle nuclei expressed GFP (Figure 3A') suggesting that they are derived from ancestral Enh3 expressing cells. Furthermore, close examination of the Enh3 driven RFP expression showed that it often persisted in two nearby muscle nuclei (Figure 3A-A'). This suggests that these nuclei are recent progeny of Enh3-expressing cells, indicating that these cells have retained the ability to divide, a characteristic of satellite cell populations (Figure 3). To further substantiate this conclusion, we verified that adult Zfh1+ve cells were actively dividing cells, using the mitotic marker phosphohistone-3 (PH3) staining. Many Zfh1+ve cells co-stained with PH3 indicating that these adult cells remain mitotically active (Figure 3B-B'').

If the mitotically active Zfh1+ve cells are indeed important for muscle homoestasis, their progeny should become incorporated into the muscle fibres. We therefore quantified the proportion of muscle nuclei derived from the pMPs during the first 10 days of the adult life, by using a temperature sensitive Gal80 (*tubGal80ts*) to restrict *Enh3-Gal4* until eclosion and combining it with the *G-Trace* cassette to mark the progeny (Figure 3C-D). Strikingly, the conditional activation of *Enh3-Gal4* in adults resulted in GFP labeling of ~24% of muscle nuclei (Figure 3D) indicating a significant role of the pMPs in contributing to muscle maintenance. Indeed when we used a similar regime to deplete *zfh1* in pMPs and examined flies at ten days (Figure 3E-I) we found that ~30% of adult flies had a "held out

wing" posture (n=93) (Figure 3E-F), a phenotype often associated with flight muscle defects (Vigoreaux, 2001). The number of nuclei per muscle (DLM4) was also significantly reduced (~ 20 % fewer nuclei) in the aged adults when *zfh1* was specifically depleted in the pMPs (Figure 3G-H). Likewise, genetic ablation of pMPs (by expressing the pro-apoptotic gene *reaper*) led to a similar reduction in muscle nuclei (Figure 3I). No "held out wing" phenotype or muscle defects were observed in adult flies within 24 hours of *zfh1* knock-down, indicating that the phenotypes at 10 days are due to a defect in the homeostasis of the adult flight muscles. Taken together the results argue that the adult Zfh1+ve myoblasts cells resemble mammalian satellite cells, retaining the capacity to divide and provide progeny that maintain the adult flight muscles.

Notch directly regulates *zfh1* expression in muscle progenitors and adults pMPs

As mentioned above, *zfh1* is regulated by Notch activity in *Drosophila* DmD8, MP-related cells (Krejci, et al., 2009), where Enh3 was bound by Su(H) (Figure 2A and Figure 2-figure supplement 1). Furthermore, phenotypes from depletion of *zfh1* in MPs, were reminiscent of those elicited by loss of Notch (N) signaling (Figure 1 and (Krejci, et al., 2009)). Notch activity is therefore a candidate to maintain Zfh1 expression in the adult pMPs, thereby preventing their premature differentiation**.** As a first step to test whether Notch activity contributes to *zfh1* expression, we depleted *Notch* in muscle progenitors by driving *Notch RNAi* expression with *1151-Gal4* (Figure 4A-C). Under these conditions, Zfh1 levels were significantly reduced, consistent with Notch being required for *zfh1* expression in MPs. Second, the consequences of perturbing Notch regulation by mutating the Su(H) binding motifs in Enh3 were analyzed. Two potential Su(H) binding sites are present in Enh3 and both are highly conserved across species (Figure 2A). Mutation of both motifs, *Enh3[mut]*, resulted in a dramatic decrease of the enhancer activity in the MPs (Figure 4D-F). This supports the hypothesis that Notch directly controls *zfh1* expression in MPs by regulating activity of Enh3.

Since Enh3 activity persists in the adult pMPs (Figure 2), we next analyzed whether mutating the Su(H) motifs impacted expression in these adult pMPs. Similar to larval stage MPs, *Enh3[mut]* had lost the ability to direct expression of GFP in the adult pMPs (Figure 4G-H). Thus, the Su(H) motifs are essential for Enh3 to be active in the adult pMPs. These data support the model that persistence of Zfh1 expression in adult MPs is likely due to Notch input, acting throughout Enh3.

The results imply that Notch should be expressed and active in the adult pMPs. To investigate this, we made use of a *Notch[NRE]-GFP* reporter line. *Notch[NRE]* is an enhancer from the *Notch* gene, and itself regulated by Notch activity, such that it is a read out both of Notch expression and of Notch activity (Simon, et al., 2014). Robust expression of *Notch[NRE]-GFP* reporter was detected in Zfh1+ve adult pMPs, confirming that Notch is active in these cells (Figure 4I) but not in the differentiated muscles. Together, the results show that *zfh1* expression in the adult pMPs requires Notch activity acting through Enh3.

zfh1 **is silenced by the conserved microRNA** ***miR-8/miR-200*** **in MPs**

Although transcriptional control of *zfh1* by Notch explains one aspect of its regulation, since all larval MPs express Zfh1 it remained unclear how a subset maintain this expression and escape from differentiation to give rise to adult pMPs. A candidate to confer an additional level of regulation on *zfh1* expression is the micro RNA *miR-8/miR-200,* which is important for silencing *zfh1* (and its mammalian homologue ZEB1) in several contexts. The regulatory loop between *miR-8/miR-200* and *zfh1/ZEB* has been extensively studied in both *Drosophila* and vertebrates and is mediated by a *miR-8/miR-200* seed site located in the 3' untranslated region (3'UTR) (Antonello, et al., 2015; Vallejo, et al., 2011; Brabletz and Brabletz, 2010). Moreover, *miR-8* was previously reported to be involved in flight muscle development (Fulga, et al., 2015).

To determine whether *miR-8* could down-regulate *zfh1* in muscle progenitors to promote their differentiation into muscles, we first examined the spatiotemporal expression pattern of *miR-8* at larval, pupal and adult stages (Figure 5) using *miR-8-Gal4,* whose activity reflects the expression of the endogenous *miR-8* promoter (Karres, et al., 2007). Expression of *miR-8-Gal4* was almost undetectable in the larval MPs, although it was highly expressed in the wing pouch (Figure 5). A low level of *miR-8-Gal4* expression was also detected in a subset of the MPs where Zfh1 levels are slightly reduced (high Ct expressing DFM precursors; Figure 5). Thus, expression of *miR-8* is inversely correlated with Zfh1; its overall expression is low in larval MPs where Zfh1 expression is important to prevent their differentiation (Figure 5B-B and Figure 1A).

We subsequently compared *miR8-Gal4* and Zfh1 expression in 18-22hr APF pupae (Figure 5D-D''). At this stage, *miR-8-Gal4* and Zfh1 expression overlapped in most, if not all, myogenic nuclei (Figure 5D). However, *miR-8-Gal4* expression level was elevated in the differentiated myoblasts, which are located inside the muscle templates (Figure 5D-D'). Conversely, Zfh1 expression level was slightly lower in this population and higher in the

undifferentiated MPs (Figure 5D-D''). Thus *miR-8* and Zfh1 have reciprocal low and high expression patterns in the MPs at this stage of myogenesis.

By 30-36hr APF, Zfh1 expression was restricted to pMPs while *miR-8-Gal4* was predominantly expressed throughout the differentiated myoblasts (Figure 5E). Notably, a few of the Zfh1+ve cells at this stage retained *miR-8-Gal4* expression (Figure 5E-E'). Similar to 30-36hr APF, adult muscles had uniform and high levels of *miR-8-Gal4* (Figure 5F-F''). However, at this time, *miR-8-Gal4* expression was totally absent from all Zfh1+ve adult pMPs (Figure 5F-F''). These data show that, during muscle formation, *miR-8* expression level is inversely correlated to Zfh1; supporting the model that *miR-8* negatively regulates *zfh1*.

Given their complementary expression patterns we next tested the impact of *miR-8* overexpression on Zfh1 protein levels in larval MPs (Figure 6A-B). Zfh1 protein levels were significantly diminished under these conditions, in agreement with *miR-8* regulating *zfh1* post-transcriptionally (Figure 6C). Although this manipulation was not sufficient to cause premature up-regulation of muscle differentiation markers or associated morphological changes in MPs, the few surviving adults all displayed a held-out wing phenotype, which is often associated with defective flight muscles (Vigoreaux, 2001). Next we assessed whether *miR-8* activity/expression changes in response to Mef2 levels, a critical determinant of muscle differentiation, using a *miR-8* sensor (containing two *miR-8* binding sites in its 3'UTR (Kennell, et al., 2012)). Expression of the *miR-8* sensor was specifically decreased when Mef2 was overexpressed in MPs, suggesting that *miR-8* expression responds to high level of Mef2 (Figure 6-figure supplement 1).

If down-regulation of *zfh1* by *miR-8* is important to allow muscle differentiation, selective depletion of *miR-8* should allow more MPs to escape differentiation. To achieve this, a *miR-8 sponge* construct (UAS-miR-8Sp (Fulga, et al., 2015) was expressed using Mef2-Gal4, so that it would decrease *miR-8* activity in differentiating myoblasts. Adult muscles were still formed under these conditions however the final number of pMPs was significantly increased (Figure 6D-F). Conversely ectopic expression of *miR-8* in adult MPs (using *Enh3-Gal4*) led to a reduction in the number of muscle nuclei similar to that seen with *zfh1* down-regulation (Figure 6-figure supplement 1D). Together, these data argue that *miR-8* up-regulation during muscle differentiation blocks Zfh1 production to allow MPs to differentiate and if its expression is compromised, more MPs are permitted to escape differentiation. It is also possible that *miR-8* has additional targets, besides Zfh1, that are involved in maintenance/differentiation of MPs.

An alternate short *zfh1* isoform is transcribed in adult pMPs

To retain their undifferentiated state, the adult pMPs must evade *miR-8* regulation and maintain Zfh1 expression. The *zfh1* gene gives rise to three different mRNA isoforms; two long *zfh1* isoforms (*zfh1-long*; *zfh1-RE/RB*) and one short *zfh1* isoform (*zfh1-short*; *zfh1-RA*) (Figure 7A). Although *zfh1-long* isoforms have two additional N-terminal zinc fingers, all three RNA-isoforms produce proteins containing the core zinc finger and homeodomains needed for Zfh1 DNA-binding activity (Figure 7-figure supplement 1 A; (Postigo, et al., 1999)). Importantly, *zfh1-short* isoform has a shorter 3'UTR, which lacks the target site for *miR-8* (Figure 7A; (Antonello, et al., 2015), as well as differing in its transcription start site (TSS) (Figure 7A; Flybase FBgn0004606). The lack of a seed site makes *zfh1-short* insensitive to *miR-8* mediated down-regulation. This means that *zfh1-short* expression would enable cells to retain high level of Zfh1 protein, even in the context of *miR-8* expression and, if present in a subset of MPs, could explaining how they can escape differentiation.

To determine whether *zfh1-short* is indeed expressed in MPs, we designed fluorescent probes specific for the *zfh1-long* and *zfh1-short* isoforms and used them for in situ hybridization (FISH) at larval and adult stages (Figure 7A). In larval stages (L3), *zfh1-long* isoforms were present at uniformly high levels in the MPs (Figure 7B-B"') whereas *zfh1-short* was expressed at much lower levels and only detected in a few MPs in each disc (Figure 7C-C"'). In adult muscles, where pMPs were marked by *Enh3-Gal4>GFP* and low Mef2 expression (Figure 7D-E), high levels of *zfh1-short* and much lower levels of *zfh1-long* (Figure 7D-E"') were present in the pMPs. Indeed, *zfh1-short* was only present in the pMPs whereas dots of *zfh1-long* hybridization were also detected in some differentiated nuclei (with high level of Mef2) (Figure 7). Thus, *zfh1-short* is expressed in a few larval MPs and is then detected at highest levels specifically in the adult pMPs but is not transcribed in adult muscle nuclei. Since *zfh1-short* is not susceptible to regulation by *miR-8*, its specific transcription may therefore be determinant for maintaining high levels of Zfh1 in a subset of progenitors and enable them to escape differentiation.

The model predicts that Zfh1-short will counteract the myogenic program in a similar manner as previously described for Zfh1-long, which antagonizes Mef2 function (Siles, et al., 2013). Premature expression of Mef2 (using *1151-Gal4*) induces precocious differentiation of larval MPs, evident by ectopic expression of *MHC-LacZ* and a reduction

of MPs (Figure 7-figure supplement 1 and ref). Expression of Zfh1-short was able to counteract the effects of Mef2, suppressing the precocious muscle differentiation phenotype and restoring the normal morphology of MPs. Thus, Zfh1-short retains the capacity to block Mef2 induced muscle differentiation (Figure 7-figure supplement 1).

zfh1-short **isoform transcription requires Notch activity in adult pMPs**

Expression of *zfh1-short* (*zfh1-RA*) is specifically retained in adult MPs (Figure 7E) where it may be critical for maintaining their progenitor status. Mechanisms that ensure this isoform is appropriately transcribed could involve Notch signaling, which is necessary for normal levels of Zfh1 expression in MPs (Figure 4). If this is the case, expression of a constitutively active Notch (Notch∆ECD) should up-regulate *zfh1-short* transcripts in the MPs at larval stages when their expression is normally low. In agreement, expression of active Notch in the progenitors (*1151-Gal4>Notch∆ECD*) significantly increased the proportions of cells transcribing *zfh1-short* (Figure 8 A-B' and C).

To address whether Notch is necessary for *zfh1-short* transcription in adult pMPs, we specifically depleted Notch levels after eclosion (using *Enh3-Gal4* in combination with *tubGal80^{ts}* to drive *Notch RNAi;* Figure 8E-F). Consistent with expression of *zfh1-short* being dependent on Notch activity, the levels of *zfh1-short* were significantly reduced in adult pMPs when Notch was down-regulated in this way (Figure 8E-F and D). Conversely, expression of *zfh1-long* isoform was less affected (Figure 8-figure supplement 1), suggesting other inputs besides Notch help to sustain *zfh1-long* in pMPs. Nevertheless, Mef2 accumulated to higher levels than normal in the adult pMPs, under these *Notch RNAi* conditions, indicating that Notch activity helps prevent their differentiation (Figure 8E', F' and H), most likely through sustaining a higher level of Zfh1 expression via its regulation of *zfh1-short*.

The increased level of Mef2 in the pMPs following Notch-depletion suggests they are losing their progenitor status and becoming differentiated. This forced differentiation of the pMPs would deplete the progenitor population and so should compromise muscle maintenance and repair. In agreement there was a significant reduction of the number of nuclei per muscle after ten days of Notch down-regulation in the pMPs (Figure 8I). These results are reminiscent of the targeted *zfh1* down-regulation in the adult pMPs (Figure 3G-H and I), where high level of Mef2 was also prematurely detected (Figure 8 G-G' and H). Taken together, the data indicate that persistent Notch activity is required to maintain *zfh1-*

short expression in pMPs, which protects the pMPs from differentiating by ensuring that sufficient Zfh1 protein is present to prevent Mef2 accumulating.

DISCUSSION

A key property of adult stem cells is their ability to remain in a quiescent state for a prolonged period of time (Li and Clevers, 2010). Investigating the maintenance of Drosophila MPs we have uncovered an important new regulatory logic, in which a switch in RNA isoforms enables a sub-population of cells to escape *miRNA* regulation and so avoid the differentiation program. At the same time, analyzing expression of a pivotal player in this regulatory loop, *zfh1*, has revealed how this mechanism sustains a population of persistent progenitors associated with adult muscles in *Drosophila*, that appear analogous to mammalian satellite cells (Figure 9).

Zfh1 maintains a population of satellite-like cells in adult Drosophila

Until recently, the fly has been thought to lack a persistent muscle stem cell population, leading to speculation about how its muscles could withstand the wear and tear of its active lifestyle. Now it emerges that expression of Zfh-1 identifies a population of muscle-associated cells in the adult that retain progenitor-like properties (Figure 9 and (Chaturvedi, et al., 2017)). Indeed we have found that Zfh-1 is critical to prevent these progenitor cells from differentiating. Its expression in the persistent adult “satellite-like” cells is dependent on a specific Zfh1 enhancer, which is directly regulated by Notch. Activity of Notch is important for maintaining Zfh1 expression and hence is required to sustain the progenitor status of these cells, similar to the situation in mammalian satellite cells, which require Notch activity for their maintenance (Mourikis and Tajbakhsh, 2014; Bjornson, et al., 2012).

Using lineage-tracing method we showed that adult Zfh1+ve cells, in normal conditions, provide new myoblasts to the fibers. Furthermore, conditional down regulation of *zfh1* led adult pMPs to enter differentiation and resulted in flight defects, evident by a held out wing posture. These results demonstrate that Zfh-1 is necessary to maintain these progenitors and that, similar to vertebrate satellite cells; the Zfh1+ve progenitor cells contribute to the adult muscles homeostasis. Others have recently shown that the pMPs are expanded in conditions of muscle injury where they are likely to contribute to repair (Chaturvedi, et al., 2017). Thus the retention of a pool of progenitor cells may be critical to maintain the physiological function of all muscles in all organism types, as also highlighted by their identification in another arthropod *Parahyle* (Alwes, et al., 2016; Konstantinides and Averof,

2014). *Drosophila* notably differs because their satellite-like cells do not express the Pax3/Pax7 homologue (*gooseberry*; data not shown), considered a canonical marker in mammals and some other organisms (Chang and Rudnicki, 2014). Nor do they express the promyogenic bHLH protein Twist (data not shown), which is present in the muscle progenitors in the embryo (Bate, et al., 1991). Instead, Zfh1 appears to fulfill an analogous function and it will be interesting to discover how widespread this alternate Zfh1 pathway is for precursor maintenance. Notably, the loss of ZEB1 in mice accelerates the temporal expression of muscle differentiation genes (e.g. MHC) suggesting that there is indeed an evolutionary conserved function of Zfh1/ZEB in regulating the muscle differentiation process (Siles, et al., 2013). This lends further credence to the model that Zfh1 could have a fundamental role in preventing differentiation that may be harnessed in multiple contexts.

Switching 3' UTR to protect progenitors from differentiation

Another key feature of *zfh-1* regulation that is conserved between mammals and flies is its sensitivity to the miR-200/miR-8 family of miRNAs (Antonello, et al., 2015; Brabletz and Brabletz, 2010). This has major significance in many cancers, where loss of miR-200 results in elevated levels of ZEB1 promoting the expansion of cancer stem cells, and has led to a widely accepted model in which the downregulation of Zfh1 family is necessary to curb stem-ness (Brabletz and Brabletz, 2010). This fits with our observations, as we find that *miR-8* is upregulated during differentiation of the MPs and suppresses Zfh1 protein expression. Critically however, only some RNA isoforms, *zfh1-long*, contain seed sites necessary for *miR-8* regulation (Antonello, et al., 2015). The alternate, *zfh1-short,* isoform has a truncated 3'UTR that lacks the *miR-8* recognition sequences and will thus be insensitive to *miR-8* regulation. Significantly, this *zfh1-short* isoform is specifically expressed in MPs that persist into adulthood and hence can help protect them from *miR-8* induced differentiation during the pupal phases when both are co-expressed. However, the pMPs remain sensitive to forced *miR-8* expression in the adult, suggesting the levels of Zfh1 are finely tuned by the expression of both *zfh1-long* and *zfh1-short*. This could be important to enable the differentiation of the MP progeny. Furthermore, the fact that Notch activity strongly promotes *zfh1-short* expression could explain how an elevated level of Notch signaling promotes expansion of pMPs following injury, as observed by others (Chaturvedi, et al., 2017).

Together the data suggest a novel molecular logic to explain the maintenance of *Drosophila* satellite-like cells. This relies on the expression of *zfh1-short,* which, by being insensitive to *miR-8* regulation, can sustain Zfh1 protein production to protect pMPs from

differentiation (Figure 9). It also implies that Notch preferentially promotes the expression of a specific RNA isoform, most likely through the use of an alternate promoter in *zfh1*. Both of these concepts have widespread implications.

Alternate use of 3'UTRs, to escape miRNA regulation, is potentially an important mechanism to tune developmental decisions. Some tissues have a global tendency to favor certain isoform types, for example, distal polyadenylation sites are preferred in neuronal tissues (Zhang, et al., 2005). Furthermore, the occurrence of alternate 3'UTR RNA isoforms is widespread (>50% human genes generate alternate 3'UTR isoforms) and many conserved *miR* target sites are contained in such alternate 3'UTRs (Tian and Manley, 2013; Sandberg, et al., 2008). Thus, similar isoform switching may underpin many instances of progenitor regulation and cell fate determination. Indeed an isoform switch appears to underlie variations in Pax3 expression levels between two different populations of muscle satellite cells in mice, where the use of alternative polyadenylation sites resulted in transcripts with shorter 3'UTRs that are resistant to regulation by *miR-206* (Boutet, et al., 2012). The selection of alternate 3'-UTRs could ensure that protein levels do not fall below a critical level (Yatsenko, et al., 2014), and in this way prevent differentiation from being triggered.

The switch in *zfh1* RNA isoforms is associated with Notch-dependent maintenance of the persistent adult MPs. Notably, *zfh1-short* is generated from an alternate promoter, as well as having a truncated 3'UTR, which may be one factor underlying this switch. Studies in yeasts demonstrate that looping occurs between promoters and polyadenylation sites, and that specific factors recruited at promoters can influence poly-A site selection (Lamas-Maceiras, et al., 2016; Tian and Manley, 2013). The levels and speed of transcription also appear to influence polyA site selection (Proudfoot, 2016; Tian and Manley, 2013; Pinto, et al., 2011). If Notch mediated activation via *Enh3* favors initiation at the *zfh1-short* promoter, this could in turn influence the selection of the proximal adenylation site to generate the truncated *miR-8* insensitive UTR. The concept that signaling can differentially regulate RNA sub-types has so far been little explored but our results suggest that is potentially of considerable significance. In future it will be important to investigate the extent that this mechanism is deployed in other contexts where signaling coordinates cell fate choices and stem cell maintenance.

458 **Materials and Methods**

Key Resources Table

Reagent type (species) or resource	Designation	Source or reference	Identifiers	Additional information
gene (D. melanogaster)	zfh1	NA	FLYB:FBgn0004606	
gene (D. melanogaster)	Notch	NA	FLYB:FBgn0004647	
gene (D. melanogaster)	miR-8	NA	FLYB:FBgn0262432	
genetic reagent (D. melanogaster)	Enh3-Gal4	Janelia Research Campus	BDSC: 49924, FLYB: FBtp0059625	FlyBase symbol: P{GMR35H09-GAL4}attP2
genetic reagent (D. melanogaster)	zfh1 RNAi (kk 103205)	Vienna Drosophila RNAi Center	VDRC : 103205	
genetic reagent (D. melanogaster)	miR-8-Gal4	Kyoto Stock Center	DGRC : 104917	Genotype : y[*] w[*]; P{w[+mW.hs]=GawB}NP5247 / CyO, P{w[-]=UAS-lacZ.UW14}UW14
genetic reagent (D. melanogaster)	UAS-miR-8-Sp	Bloomington Stock Center	BDSC: 61374, FLYB: FBst0061374	Genotype : P{UAS-mCherry.mir-8.sponge.V2}attP40/CyO; P{UAS-mCherry.mir-8.sponge.V2}attP2
genetic reagent (D. melanogaster)	Enh3-GFP	This paper		
genetic reagent (D. melanogaster)	ΔEnh3	This paper		
genetic reagent (D. melanogaster)	UAS-zfh1-short	This paper		UAS-Zfh1-short construct provided by BDGP , Clone # UF5607
genetic reagent (D. melanogaster)	Notch[NRE]-GFP	Sarah Bray (Cambridge, UK)		
antibody	anti-Zfh1	Ruth Leahmann (New York, USA)		
antibody	anti-Mef2	Eileen Furlong (Heidelberg, Germany)		
recombinant DNA reagent	pCFD4	Addgene	Addgene # 49411	
recombinant DNA reagent	pDsRed-attP	Addgene	Addgene # 51019	

***Drosophila Genetics*.** All *Drosophila melanogaster* stocks were grown on standard medium at 25°C. The following stains were used: w^{118} as wild type (wt), *UAS-white-RNAi* as control for *RNAi* experiments (BL35573), *UAS-zfh1-RNAi* (VDRC: KK103205, TRiP: BL29347), *zfh1* deficiency (BL7917), Mef2-*Gal4* (Ranganayakulu, et al., 1996), *UAS-Mef2* (Cripps, et al., 2004), *UAS-G-Trace* (BL28281), *UAS-Notch-RNAi* (BL7078), *Notch[NRE]-GFP* (Simon, et al., 2014), *UAS-Notch∆ECD* (Chanet, et al., 2009; Fortini and Artavanis-Tsakonas, 1993; Rebay, et al., 1993), *miR8-Gal4* (Karres, et al., 2007), *UAS-miR-8* (Vallejo, et al., 2011)*, UAS-miR-8-Sp* (BL61374 and (Fulga, et al., 2015)), *UAS-Scramble-SP* (BL61501), *UAS-mCD8::GFP* (BL5137), *UAS-GFPnls* (BL65402), *UAS-Src::GFP* (Kaltschmidt, et al., 2000), *MHC-lacZ* (Hess et al., 1989), *1151-Gal4* (Anant, et al., 1998), *miR-8-sensor-EGFP* (Kennell, et al., 2012), *CG9650-LacZ* (Ahmad, et al., 2014), *UAS-Reaper* (BL5824). Enhancer-Gal4 lines described in Figure 2 and Figure 2-figure supplement 1 are either from Janelia FlyLight (http://flweb.janelia.org) or Vienna Tiles Library (http://stockcenter.vdrc.at/control/main).

RNAi experiments were conducted at 29°C. For adult specific manipulations in pMPs *tubGal80ts* (McGuire, et al., 2003) was used to limit *Enh3-Gal4* expression to a defined period of time. Crosses were kept at 18°C and eclosed adults were shifted to 29°C until dissection.

***Immunohistochemistry and in situ hybridization*.** Immunofluorescence stainings of wing discs were performed using standard techniques. Dissection and staining of the pupal muscles was performed according to (Weitkunat and Schnorrer, 2014). Adult muscles were prepared and stained as described in (Hunt and Demontis, 2013). The following primary antibody were used: Rabbit anti-Zfh1 (1:5000, a gift from Ruth Lehmann, New York, USA), Mouse anti-Cut (1:20, DSHB), Rabbit anti-β3-Tubulin (1:5000, a gift from Renate Renkawitz-Pohl, Marburg, Germany), Rat anti-Tropomyosin (1:1000, Abcam, ab50567), Goat anti-GFP (1:200, Abcam, ab6673), Rabbit anti-Ds-Red (1:25; Clontech, 6324496), Rabbit anti-Mef2 (1:200, a gift from Eileen Furlong, Heidelberg, Germany), Mouse anti-P1 (1:20, a gift from István Andó, Szeged, Hugary), Mouse anti-PH3 (1:100, Cell Signaling Technology, #9706), Mouse anti-β-Gal (1:1000, Promega, Z378A), Alexa-conjugated Phalloidin (1:200, Thermo fisher), Rat anti-Dcad2 (1:200, DSHB). *In situ* experiments were carried out according to Stellaris-protocols (https://www.biosearchtech.com/assets/bti_custom_stellaris_drosophila_protocol.pdf). Antibodies were included to the overnight hybridization step (together with the probes).

zfh1 probes were generated by Bioresearch Technologies. The sequence used for *zfh1-short* probe span 393bp of the first zfh1-RA exon, for *zfh1-long* probe, the sequence of the third exon (711bp) common to both zfh1-RB and zfh1-RE was used (see Figure 5).

Construction of transgenic lines and mutagenesis. For Enh3-GFP reporter line, the genomic region chr3R: 30774595..30778415 (Enh3/GMR35H09) according to Flybase genome release r6.03 was amplified using *yw* genomic DNA as template. Enh3 fragment was then cloned into the pGreenRabbit vector (Housden, et al., 2012). For *Enh3[mut]-GFP* line, two Su(H) biding sites were predicted within Enh3 sequence using Patser (Hertz and Stormo, 1999) and mutated by PCR based approach with primers overlapping the Su(H) sites to be mutated with the following sequence modifications : Su(H)1 AGTGGGAA to AGGTGTGA and Su(H) 2 TTCTCACA to TGTTTGCA. Both constructs were inserted into an AttP located at 68A4 on chromosome III by injection into *nos-phiC31-NLS; attP2* embryos (Bischof, et al., 2007). The UAS-Zfh1-Short transgenic line (Figure 7-figure supplement 1) was similarly generated using phiC mediated integration of an AttB plasmid carrying UAS-Zfh1-Short (BDGP Clone # UF5607) into an AttP site at position 25C7. The transgene produced detectable nuclear Zfh1 protein when crossed to Gal4 driver lines (data not shown). All constructs were fully sequenced and analyzed prior to injection.

CRISPR/Cas9 genome editing. CRISPR mediated deletion of Enh3 was performed according to (Port, et al., 2014). For generating guide RNAs, two protospacers were selected (sgRNA1 GCATTCCGCAGGTTTAGTCAC and sgRNA2 GCGATAACCCGGCGACCTCC) flanking 5' and 3' Enhancer-3 regions, (http://www.flyrnai.org/crispr/). The protospacers were cloned into the tandem guide RNA expression vector pCFD4 (Addgene #49411) (http://www.crisprflydesign.org/wp-content/uploads/2014/06/Cloning-with-pCFD4.pdf). For the homology directed repair step, two homology arms were amplified using *yw* genomic DNA as template with the following primers (Homology arm1: Fwd. 5' GCGCGAATTCGGGCTAAACGCCAGATAAGCG 3' Rev. 5' TTCCGCGGCCGCCACTGGATTCCACGGCTTTTCG 3'– Homology arm 2: Fwd. 5' GGTAGCTCTTCTTATATAACCCGGCGACCTCCTCG3'- Rev. 5'GGTAGCTCTTCTGACC GGACGAAAAACTAGCGACC) and cloned into the pDsRed-attP (Addgene #51019) vector (http://flycrispr.molbio.wisc.edu/protocols/pHD-DsRed-attP). Both constructs were injected into *nos-Cas9* (BL54591) embryos. Flies mutant for Enhancer 3 were screened for the expression of the Ds-Red in the eyes and confirmed with sequencing of PCR fragment spanning the deletion. ΔEhn3 was then crossed to strains carrying a deletion (BL7917),

which removes *zfh1*. None of the tranheterozygote animals survived to adults confirming that ΔEhn3 lethality maps to the *zfh1* locus.

Microscopy and data analysis. Samples were imaged on Leica SP2 or TCS SP8 microscopes (CAIC, University of Cambridge) at 20X or 40X magnification and 1024/1024 pixel resolution. Images were processed with Image J and assembled with Adobe Illustrator. Quantification of fluorescence signal intensities was performed with Image J software. In each case the n refers to the number of individual specimens analyzed, which were from two or more independent experiments. For experiments to compare and measure expression levels, samples were prepared and analyzed in parallel, with identical conditions and the same laser parameters used for image acquisition. For each confocal stack a Sum slices projections was generated. Signal intensities were obtained by manually outlining the regions of interest, based on expression of markers, and measuring the average within each region. The values were then normalized to similar background measurements for each sample. In Figure 8 the number of transcriptional *zfh1-short* dots was counted manually with Image J and normalized to the total number of nuclei (Zfh1 staining), which was determined by a Matlab homemade script. Graphs and statistical analysis were performed with Prism 7 using unpaired t-test. Error bars indicate standard error of the mean. Further statistical details of experiments can be found in the figure legends.

Quantitative RT PCR. 30 Wing Imaginal discs from each genotype were dissected and RNA isolated using TRIzol (Life technologies). Quantitative PCR were performed as described (Krejci and Bray, 2007). Values were normalized to the level of *Rpl32*. The following primers were used. *Rpl32,* Fwd 5'-ATGCTAAGCTGTCGCACAAATG-3' and Rev 5'-GTTCGATCCGTAACCGATGT-3'. *zfh1* Fwd 5'- GTTCAAGCACCACCTCAAGGAG-3' and Rev 5'- CTTCTTGGAGGTCATGTGGGAGG-3'. (Product common to all three *zfh1* isoforms).

Acknowledgements

We acknowledge the Bloomington Stock Center, the VDRC Stock Center and the Developmental Studies Hybridoma Bank for *Drosophila* strains and antibodies. We thank Ruth Lehmann, Renate Renkawitz-Pohl, Eileen Furlong and István Andó for antibodies. We thank Eva Zacharioudaki, Alain Vincent and Michalis Averof for critical reading of the manuscript and other members of SJB lab for valuable discussion; and we are grateful to Hannah Green and Juanjo Perez-Moreno for advice on muscle preparations. This work was funded by a program grant from the MRC to SJB and by an EMBO Long Term Fellowship for HB.

Competing interest

The authors declare that they have no competing interests.

REFERENCES

Ahmad, S.M., Busser, B.W., Huang, D., Cozart, E.J., Michaud, S., Zhu, X., Jeffries, N., Aboukhalil, A., Bulyk, M.L., Ovcharenko, I., et al. (2014). Machine learning classification of cell-specific cardiac enhancers uncovers developmental subnetworks regulating progenitor cell division and cell fate specification. Development 141, 878-88.10.1242/dev.101709

Alwes, F., Enjolras, C., and Averof, M. (2016). Live imaging reveals the progenitors and cell dynamics of limb regeneration. Elife 5.10.7554/eLife.19766

Anant, S., Roy, S., and VijayRaghavan, K. (1998). Twist and Notch negatively regulate adult muscle differentiation in Drosophila. Development 125, 1361-9

Antonello, Z.A., Reiff, T., Ballesta-Illan, E., and Dominguez, M. (2015). Robust intestinal homeostasis relies on cellular plasticity in enteroblasts mediated by miR-8-Escargot switch. EMBO J 34, 2025-41.10.15252/embj.201591517

Aradhya, R., Zmojdzian, M., Da Ponte, J.P., and Jagla, K. (2015). Muscle niche-driven Insulin-Notch-Myc cascade reactivates dormant Adult Muscle Precursors in Drosophila. Elife 4.10.7554/eLife.08497

Bate, M., Rushton, E., and Currie, D.A. (1991). Cells with persistent twist expression are the embryonic precursors of adult muscles in Drosophila. Development 113, 79-89

Benlhabib, H., Guo, W., Pierce, B.M., and Mendelson, C.R. (2015). The miR-200 family and its targets regulate type II cell differentiation in human fetal lung. J Biol Chem 290, 22409-22.10.1074/jbc.M114.636068

Bernard, F., Dutriaux, A., Silber, J., and Lalouette, A. (2006). Notch pathway repression by vestigial is required to promote indirect flight muscle differentiation in Drosophila melanogaster. Dev Biol 295, 164-77.10.1016/j.ydbio.2006.03.022

Bernard, F., Krejci, A., Housden, B., Adryan, B., and Bray, S.J. (2010). Specificity of Notch pathway activation: twist controls the transcriptional output in adult muscle progenitors. Development 137, 2633-42.10.1242/dev.053181

Bischof, J., Maeda, R.K., Hediger, M., Karch, F., and Basler, K. (2007). An optimized transgenesis system for Drosophila using germ-line-specific phiC31 integrases. Proc Natl Acad Sci U S A 104, 3312-7.10.1073/pnas.0611511104

Bjornson, C.R., Cheung, T.H., Liu, L., Tripathi, P.V., Steeper, K.M., and Rando, T.A. (2012). Notch signaling is necessary to maintain quiescence in adult muscle stem cells. Stem Cells 30, 232-42.10.1002/stem.773

Boutet, S.C., Cheung, T.H., Quach, N.L., Liu, L., Prescott, S.L., Edalati, A., Iori, K., and Rando, T.A. (2012). Alternative polyadenylation mediates microRNA regulation of muscle stem cell function. Cell Stem Cell 10, 327-36.10.1016/j.stem.2012.01.017

602 Brabletz, S., and Brabletz, T. (2010). The ZEB/miR-200 feedback loop--a motor of cellular
603 plasticity in development and cancer? EMBO Rep 11, 670-7.10.1038/embor.2010.117
604 Chanet, S., Vodovar, N., Mayau, V., and Schweisguth, F. (2009). Genome engineering-
605 based analysis of Bearded family genes reveals both functional redundancy and a
606 nonessential function in lateral inhibition in Drosophila. Genetics 182, 1101-
607 8.10.1534/genetics.109.105023
608 Chang, N.C., and Rudnicki, M.A. (2014). Satellite cells: the architects of skeletal muscle.
609 Curr Top Dev Biol 107, 161-81.10.1016/B978-0-12-416022-4.00006-8
610 Chaturvedi, D., Reichert, H., Gunage, R.D., and VijayRaghavan, K. (2017). Identification
611 and functional characterization of muscle satellite cells in Drosophila. Elife
612 6.10.7554/eLife.30107
613 Cripps, R.M., Lovato, T.L., and Olson, E.N. (2004). Positive autoregulation of the Myocyte
614 enhancer factor-2 myogenic control gene during somatic muscle development in
615 Drosophila. Dev Biol 267, 536-47.10.1016/j.ydbio.2003.12.004
616 Elgar, S.J., Han, J., and Taylor, M.V. (2008). mef2 activity levels differentially affect gene
617 expression during Drosophila muscle development. Proc Natl Acad Sci U S A 105, 918-
618 23.10.1073/pnas.0711255105
619 Evans, C.J., Olson, J.M., Ngo, K.T., Kim, E., Lee, N.E., Kuoy, E., Patananan, A.N., Sitz, D.,
620 Tran, P., Do, M.T., et al. (2009). G-TRACE: rapid Gal4-based cell lineage analysis in
621 Drosophila. Nat Methods 6, 603-5.10.1038/nmeth.1356
622 Fernandes, J., Bate, M., and Vijayraghavan, K. (1991). Development of the indirect flight
623 muscles of Drosophila. Development 113, 67-77
624 Figeac, N., Daczewska, M., Marcelle, C., and Jagla, K. (2007). Muscle stem cells and
625 model systems for their investigation. Dev Dyn 236, 3332-42.10.1002/dvdy.21345
626 Figeac, N., Jagla, T., Aradhya, R., Da Ponte, J.P., and Jagla, K. (2010). Drosophila adult
627 muscle precursors form a network of interconnected cells and are specified by the
628 rhomboid-triggered EGF pathway. Development 137, 1965-73.10.1242/dev.049080
629 Fortini, M.E., and Artavanis-Tsakonas, S. (1993). Notch: neurogenesis is only part of the
630 picture. Cell 75, 1245-7
631 Fulga, T.A., McNeill, E.M., Binari, R., Yelick, J., Blanche, A., Booker, M., Steinkraus, B.R.,
632 Schnall-Levin, M., Zhao, Y., DeLuca, T., et al. (2015). A transgenic resource for conditional
633 competitive inhibition of conserved Drosophila microRNAs. Nat Commun 6,
634 7279.10.1038/ncomms8279
635 Gunage, R.D., Reichert, H., and VijayRaghavan, K. (2014). Identification of a new stem
636 cell population that generates Drosophila flight muscles. Elife 3.10.7554/eLife.03126

637 Hertz, G.Z., and Stormo, G.D. (1999). Identifying DNA and protein patterns with
638 statistically significant alignments of multiple sequences. Bioinformatics 15, 563-77
639 Housden, B.E., Millen, K., and Bray, S.J. (2012). Drosophila Reporter Vectors Compatible
640 with PhiC31 Integrase Transgenesis Techniques and Their Use to Generate New Notch
641 Reporter Fly Lines. G3 (Bethesda) 2, 79-82.10.1534/g3.111.001321
642 Hunt, L.C., and Demontis, F. (2013). Whole-mount immunostaining of Drosophila skeletal
643 muscle. Nat Protoc 8, 2496-501.10.1038/nprot.2013.156
644 Jenett, A., Rubin, G.M., Ngo, T.T., Shepherd, D., Murphy, C., Dionne, H., Pfeiffer, B.D.,
645 Cavallaro, A., Hall, D., Jeter, J., et al. (2012). A GAL4-driver line resource for Drosophila
646 neurobiology. Cell Rep 2, 991-1001.10.1016/j.celrep.2012.09.011
647 Jory, A., Estella, C., Giorgianni, M.W., Slattery, M., Laverty, T.R., Rubin, G.M., and Mann,
648 R.S. (2012). A survey of 6,300 genomic fragments for cis-regulatory activity in the imaginal
649 discs of Drosophila melanogaster. Cell Rep 2, 1014-24.10.1016/j.celrep.2012.09.010
650 Kaltschmidt, J.A., Davidson, C.M., Brown, N.H., and Brand, A.H. (2000). Rotation and
651 asymmetry of the mitotic spindle direct asymmetric cell division in the developing central
652 nervous system. Nat Cell Biol 2, 7-12.10.1038/71323
653 Karres, J.S., Hilgers, V., Carrera, I., Treisman, J., and Cohen, S.M. (2007). The conserved
654 microRNA miR-8 tunes atrophin levels to prevent neurodegeneration in Drosophila. Cell
655 131, 136-45.10.1016/j.cell.2007.09.020
656 Kennell, J.A., Cadigan, K.M., Shakhmantsir, I., and Waldron, E.J. (2012). The microRNA
657 miR-8 is a positive regulator of pigmentation and eclosion in Drosophila. Dev Dyn 241,
658 161-8.10.1002/dvdy.23705
659 Konstantinides, N., and Averof, M. (2014). A common cellular basis for muscle
660 regeneration in arthropods and vertebrates. Science 343, 788-
661 91.10.1126/science.1243529
662 Korpal, M., Lee, E.S., Hu, G., and Kang, Y. (2008). The miR-200 family inhibits epithelial-
663 mesenchymal transition and cancer cell migration by direct targeting of E-cadherin
664 transcriptional repressors ZEB1 and ZEB2. J Biol Chem 283, 14910-
665 4.10.1074/jbc.C800074200
666 Krejci, A., Bernard, F., Housden, B.E., Collins, S., and Bray, S.J. (2009). Direct response
667 to Notch activation: signaling crosstalk and incoherent logic. Sci Signal 2,
668 ra1.10.1126/scisignal.2000140
669 Krejci, A., and Bray, S. (2007). Notch activation stimulates transient and selective binding
670 of Su(H)/CSL to target enhancers. Genes Dev 21, 1322-7.10.1101/gad.424607

671 Lamas-Maceiras, M., Singh, B.N., Hampsey, M., and Freire-Picos, M.A. (2016). Promoter-
672 Terminator Gene Loops Affect Alternative 3'-End Processing in Yeast. J Biol Chem 291,
673 8960-8.10.1074/jbc.M115.687491
674 Li, L., and Clevers, H. (2010). Coexistence of quiescent and active adult stem cells in
675 mammals. Science 327, 542-5.10.1126/science.1180794
676 Manning, L., Heckscher, E.S., Purice, M.D., Roberts, J., Bennett, A.L., Kroll, J.R., Pollard,
677 J.L., Strader, M.E., Lupton, J.R., Dyukareva, A.V., et al. (2012). A resource for
678 manipulating gene expression and analyzing cis-regulatory modules in the Drosophila
679 CNS. Cell Rep 2, 1002-13.10.1016/j.celrep.2012.09.009
680 McGuire, S.E., Le, P.T., Osborn, A.J., Matsumoto, K., and Davis, R.L. (2003).
681 Spatiotemporal rescue of memory dysfunction in Drosophila. Science 302, 1765-
682 8.10.1126/science.1089035
683 Mourikis, P., Gopalakrishnan, S., Sambasivan, R., and Tajbakhsh, S. (2012). Cell-
684 autonomous Notch activity maintains the temporal specification potential of skeletal
685 muscle stem cells. Development 139, 4536-48.10.1242/dev.084756
686 Mourikis, P., and Tajbakhsh, S. (2014). Distinct contextual roles for Notch signalling in
687 skeletal muscle stem cells. BMC Dev Biol 14, 2.10.1186/1471-213X-14-2
688 Park, S.M., Gaur, A.B., Lengyel, E., and Peter, M.E. (2008). The miR-200 family
689 determines the epithelial phenotype of cancer cells by targeting the E-cadherin repressors
690 ZEB1 and ZEB2. Genes Dev 22, 894-907.10.1101/gad.1640608
691 Pinto, P.A., Henriques, T., Freitas, M.O., Martins, T., Domingues, R.G., Wyrzykowska,
692 P.S., Coelho, P.A., Carmo, A.M., Sunkel, C.E., Proudfoot, N.J., et al. (2011). RNA
693 polymerase II kinetics in polo polyadenylation signal selection. EMBO J 30, 2431-
694 44.10.1038/emboj.2011.156
695 Port, F., Chen, H.M., Lee, T., and Bullock, S.L. (2014). Optimized CRISPR/Cas tools for
696 efficient germline and somatic genome engineering in Drosophila. Proc Natl Acad Sci U S
697 A 111, E2967-76.10.1073/pnas.1405500111
698 Postigo, A.A., Ward, E., Skeath, J.B., and Dean, D.C. (1999). zfh-1, the Drosophila
699 homologue of ZEB, is a transcriptional repressor that regulates somatic myogenesis. Mol
700 Cell Biol 19, 7255-63
701 Proudfoot, N.J. (2016). Transcriptional termination in mammals: Stopping the RNA
702 polymerase II juggernaut. Science 352, aad9926.10.1126/science.aad9926
703 Ranganayakulu, G., Schulz, R.A., and Olson, E.N. (1996). Wingless signaling induces
704 nautilus expression in the ventral mesoderm of the Drosophila embryo. Dev Biol 176, 143-
705 8.10.1006/dbio.1996.9987

Rebay, I., Fehon, R.G., and Artavanis-Tsakonas, S. (1993). Specific truncations of Drosophila Notch define dominant activated and dominant negative forms of the receptor. Cell 74, 319-29

Roy, S., and VijayRaghavan, K. (1998). Patterning muscles using organizers: larval muscle templates and adult myoblasts actively interact to pattern the dorsal longitudinal flight muscles of Drosophila. J Cell Biol 141, 1135-45

Sandberg, R., Neilson, J.R., Sarma, A., Sharp, P.A., and Burge, C.B. (2008). Proliferating cells express mRNAs with shortened 3' untranslated regions and fewer microRNA target sites. Science 320, 1643-7.10.1126/science.1155390

Siles, L., Sanchez-Tillo, E., Lim, J.W., Darling, D.S., Kroll, K.L., and Postigo, A. (2013). ZEB1 imposes a temporary stage-dependent inhibition of muscle gene expression and differentiation via CtBP-mediated transcriptional repression. Mol Cell Biol 33, 1368-82.10.1128/MCB.01259-12

Simon, R., Aparicio, R., Housden, B.E., Bray, S., and Busturia, A. (2014). Drosophila p53 controls Notch expression and balances apoptosis and proliferation. Apoptosis 19, 1430-43.10.1007/s10495-014-1000-5

Sudarsan, V., Anant, S., Guptan, P., VijayRaghavan, K., and Skaer, H. (2001). Myoblast diversification and ectodermal signaling in Drosophila. Dev Cell 1, 829-39

Tian, B., and Manley, J.L. (2013). Alternative cleavage and polyadenylation: the long and short of it. Trends Biochem Sci 38, 312-20.10.1016/j.tibs.2013.03.005

Vallejo, D.M., Caparros, E., and Dominguez, M. (2011). Targeting Notch signalling by the conserved miR-8/200 microRNA family in development and cancer cells. EMBO J 30, 756-69.10.1038/emboj.2010.358

Vandewalle, C., Van Roy, F., and Berx, G. (2009). The role of the ZEB family of transcription factors in development and disease. Cell Mol Life Sci 66, 773-87.10.1007/s00018-008-8465-8

Vigoreaux, J.O. (2001). Genetics of the Drosophila flight muscle myofibril: a window into the biology of complex systems. Bioessays 23, 1047-63.10.1002/bies.1150

Weitkunat, M., and Schnorrer, F. (2014). A guide to study Drosophila muscle biology. Methods 68, 2-14.10.1016/j.ymeth.2014.02.037

Yatsenko, A.S., Marrone, A.K., and Shcherbata, H.R. (2014). miRNA-based buffering of the cobblestone-lissencephaly-associated extracellular matrix receptor dystroglycan via its alternative 3'-UTR. Nat Commun 5, 4906.10.1038/ncomms5906

Zaravinos, A. (2015). The Regulatory Role of MicroRNAs in EMT and Cancer. J Oncol 2015, 865816.10.1155/2015/865816

741 Zhang, H., Lee, J.Y., and Tian, B. (2005). Biased alternative polyadenylation in human
742 tissues. Genome Biol 6, R100.10.1186/gb-2005-6-12-r100

743 **FIGURE LEGENDS:**

744 **Figure 1. Zfh1 expression and function in MPs and in adult pMPs. (A-A'')** Zfh1
745 (Green) and Cut (Purple) expression in MPs associated with third instar wing discs, (**A'-**
746 **A''**) higher magnification (3X) of boxed region in A. Zfh1 is present in all MPs, but those
747 with highest Cut expression have lower levels of Zfh1 (asterisk). Scale bars: 50 μM, (n>30

wing discs from three biological replicates). (**B-C)** Down regulation of *zfh1* induces premature differentiation of the MPs (arrowhead in C'-C''). β3-Tubulin (β3-Tub, Red) and Tropomyosin (Tm, Green) expression in control (B, *1151-Gal4>wRNAi*) and Zfh1 depleted (C, *1151-Gal4>zfh1RNAi*) third instar wing discs, (B'-C'') higher magnification (3X) of boxed regions in B and C. (n>20 wing discs; from three biological replicates). (**D-D'**) Zfh1 expression (red) indicates the existence of persistent muscle progenitors (pMPs; arrows) associated with the muscle fibres (Phalloidin (Green), DNA/Nuclei (Blue); n>10 heminota; from three biological replicates). The immune cell marker P1 was included in the immunostaining and is absent from the pMPs (see Figure 1-figure supplement 2). Scale bars: 50 μM. (**E-E'''**) Zfh1 (Red) expressing pMPs (e.g. arrows in E''') are closely embedded in the muscle lamina of the adult indirect flight muscles and express Mef2 (myogenic cells; *Mef2>Src::GFP, green*). Nuclei (Blue), Scale bars: 25μM, (n>10 heminota; from two biological replicates).

Figure 1-figure supplement 1. (A) Zfh1 (Green) expression in MPs associated with early third instar wing discs showing that at this stage Zfh1 is uniformly expressed in all the MPs. Scale bar: 50μM. **(B)** Third instar wing discs stained for Zfh1 (Green), PH3 (Red) and Dcad2 (Blue) revealing that some MPs are undertaking mitotic divisions. Scale bar: 50 μM**.** (n=12 wing discs from two biological replicates). **(C-C')** Optical section of image B showing active mitotic division of Zfh1 MPs in the most proximal layer to the disc epithelium (Arrows). Scale bar: 25μM. **(D-E)** Zfh1 (Green), β-Gal (CG9650-LacZ, Red, marks MPs) and DAPI (Blue) expression in control (D, *1151-Gal4; CG9650-LacZ >white-RNAi*) and *zfh1* down regulation (*1151-Gal4>zfh1-RNAi*) with KK 103205 RNAi line. Scale bars: 50 μM. The level of Zfh1 protein is strongly reduced after *zfh1 RNAi* expression in the MPs (D'' and E''). **(F-G)** β3-Tubulin (β-Tub, Red) and Tropomyosin (Green) expression in control (F, *1151-Gal4>white-RNAi*) and *zfh1* down regulation (*1151-Gal4>zfh1-RNAi)* with the Val10 TRiP RNAi line. Premature differentiation of MPs is observed using the TRiP Val10 *zfh1* RNAi line comparing to the control (arrow; n>10 wing discs for each genotype from two biological replicates). **(H-I)** β3-Tubulin (β-Tub, Red) and *MHC-lacZ* (Green) expression in control (H, *1151-Gal4; MHC-lacZ>white-RNAi*) and *zfh1* down regulation (I, *1151-Gal4; MHC-lacZ>zfh1-RNAi)* with the KK 103205 RNAi line. Premature differentiation of the MPs is observed by the expression of *MHC-LacZ* reporter line after *zfh1* down regulation (n=20 wing discs from two biological replicates).

Figure 1-figure supplement 2. (A-A'') Wild type indirect flight muscles stained for P1

(Cyan), Zfh1 (Red), Phalloidin (Green) and DAPI (Blue). P1 expression indicates the presence of phagocytic immune cells, which are also positive for Zfh1. Insets: boxed regions magnified 4X. Scale bar: 50 μM. (n=27 heminota from two biological replicates). **(B-B'')** Indirect flight muscles from flies expressing *Mef2-Gal4>UAS-GFPnls* stained for GFP (Green), P1 (Blue), Zfh1 (Red) and Phalloidin (Cyan). The Zfh1 immune cells detected in the IFMs lack Mef2 expression (Arrows B-B''). Scale bar: 25μM**.** (n=11 heminota from two biological replicates)**.**

Figure 2. Regulation of *zfh1* in MPs and adult pMPs. (A) Schematic view of *zfh1* genomic region, *zfh1* regulatory enhancers are represented by green rectangles and arrows indicate transcription start-sites. Coding exons and untranslated regions are represented in black and grey boxes, respectively. (**B-D)** Three different *zfh1* enhancers are active in the MPs (labelled with Cut, purple). *Enh1* (VT050105, B) drives GFP (Green) in a subset of scattered MPs; *Enh2* (VT050115, C) drives GFP throughout the MPs, and in some non-MP cells (asterisk); *Enh3* (GMR35H09, D) is highly expressed in a subset of MPs located in the posterior region of the notum. Scale bars: 50 μM. (n=30 wing discs). **(E-E'')** *Enh3-GFP* (Green) expression is maintained in adult pMPs (characterised by low levels of Mef2, red; arrows E'-E'') but not in differentiated muscle nuclei (high Mef2, red; arrowheads G'-G''). Phalloidin marks muscles (Cyan) and DAPI labels all nuclei (Blue). Insets: boxed regions magnified 12.5 X. Scale bars 25 μM. (n=10 heminota; from two biological replicates). (**F-G)** Muscle (IFM) preparation isolated from *Enh3-Gal4>UAS-GFP* pupae at 18-22hr APF (F) or at 30-36hr APF (G). Enh3 (Green) and Zfh1 (Red) are detected in MPs. (F) At 18-22hr Enh3 activity is higher (arrowheads in E') in some undifferentiated MPs located between muscle templates (muscles are labeled with Phalloidin, Blue, asterisks). **(G)** At 30-36hr APF, Enh3 (Green) activity and Zfh1 (Red) are detected in pMPs (arrowheads) and not in differentiated muscle nuclei. A few Zfh1+ve cells do not express Enh3 (Arrows G''). Note: anti-P1, an immune cell marker, was included in the staining to exclude plasmatocytes from the analysis (see Figure 1-figure supplement 2)**.**

Figure 2-figure supplement 1. (A) Identification of active *zfh1* enhancers in MPs and pMPs. Chromosome 3R: 30,765,926-30,789,202 showing the *zfh1* genomic region with coding exons and untranslated regions represented in black and grey boxes, respectively. Arrows represent the transcription start-sites. Su (H) and Twi ChIP enriched regions in

DmD8 cells are represented in Blue and Purple, respectively (Data from Bernard et al.,2010 (ChIP Twi) and Krejci et al., 2009 (ChIP Su(H)). Black lines represent all GMR and VT lines tested in our study. Green lines indicate the enhancers that are active in MPs *in vivo*. **(B-D)** Zfh1 (white) expression in MPs is significantly reduced in discs from *Enh3* deletion ∆*Enh3* (C) compared to controls (B). In each condition light and dark shading indicates data points from two independent replicates (* $p<0.05$, Student t-test; n=14 wing discs for each genotype). Scale bars: 50 µM. **(E)** Effect of Enh3 deletion (*ΔEnh3*) on *zfh1* mRNA level in MPs as determined by quantitative RT-PCR. *zfh1* mRNA level is significantly decreased by Enh3 deletion. ** $p=0.0042$ was obtained using unpaired Student's t-test. Error bars represent s.e.m of three independent experiments.

Figure 3. Adult pMPs contribute to muscle homeostasis. (A-A'') Lineage tracing shows that adult pMPs contribute to muscles. Cross-section of indirect flight muscles from adult flies where *Enh3-Gal4* drives expression of the *G-Trace* cassette; GFP (Green) indicates myoblasts that have expressed Enh3-Gal4, RFP (Red) indicates myoblasts where Gal4 is still active, Mef2 labels muscle nuclei (Blue). Note that the RFP (Red, detected with anti-RFP in A') persists in the recently born myoblasts (Mef2), which are closely localized to the pMPs. Insets: boxed regions magnified 20 X (n=15 heminota; from three biological replicates). (**B-B''**) pMPs are mitoticaly active, indicated by anti-phosphH3 (White in B''). (PH3 detected in 47 % of pMPs, n= 80; from three biological replicates). **(C-C'')** Cross-section of indirect flight muscles from adult flies (*Enh3-Gal4; tubGal80ts>G-Trace)* where *Enh3-Gal4* directed *G-Trace* activity was induced for 10 days after animal hatching. GFP (Green, Arrowheads, C') indicates descendants of pMPs (Blue, Arrows); Mef2 labels muscle nuclei (Red, White). **(D)** Proportion of newly born myoblasts (marked by GFP; e.g. C') relative to total number of myoblasts (marked by Mef2; e.g. C'') in muscle preparations. (n=18 heminota; light and dark shading indicates data points collected from two independent replicates replicates). Scale bar: 60µM. **(E-F)** Prolonged *zfh1* depletion in pMPs (10 days after adult hatching) leads to a "held out" wings posture; dorsal view of (E) control (*Enh3-Gal4; tubGal80ts > UAS-wRNAi;*) and (F) *zfh1* depletion (*Enh3-Gal4; tubGal80ts > UAS-zfh1RNAi* (KK 103205)) adult flies. **(G-H)** Transverse sections of DLM4 muscle stained with Phalloidin (Green) and Mef2 (Red, White) from the indicated genotypes. Fewer Mef2+ve nuclei are present in muscles when *zfh1* is depleted. Scale bars: 50 µM. **(I)**. Similar reductions in muscle nuclei occur following *zfh1* depletion (*Enh3-Gal4; tubGal80ts >UAS-zfh1RNAi*) or following genetic ablation of pMPs, via expression of the pro-apoptotic gene *reaper* (*rpr; Enh3-Gal4;tubGal80ts>UAS-rpr*). The number of nuclei

per section in the indicated conditions was significantly different, light and dark shading indicates data points collected from two independent replicates (>*zfh1 RNAi* ***p=0.0013, n=16; >*Rpr* ***p<0.0001, n=12).

Figure 4. Notch directs Zfh1 expression in MPs and pMPs. (A-C) Zfh1 level (White) is significantly reduced when *Notch* is down regulated. Expression of Zfh1 in MPs (A) is severely reduced in the presence of *Notch* RNAi (B, *1151-Gal4>UAS-NotchRNAi*), Scale Bars: 50 μM. (C) Quantification of Zfh1 expression levels (*p<0.05, n=12 wing discs in each condition, light and dark shading indicates data obtained from two independent replicates). (**D-F)** *Enh3* (D, *Enh3-GFP*, Green) expression in MPs (Purple, Zfh1) is abolished when Su(H) motifs are mutated (E, *Enh3[mut]-GFP*). Scale bars: 50 μM. (F) Quantification of expression from *Enh3* and *Enh3[mut]* (*p=0.022, n=14 wing discs in each condition, light and dark shading indicates data obtained from two independent replicates). (**G-H)** *Enh3* (G, *Enh3-GFP*, Green) expression in adult pMPs (red, Zfh1) is abolished when Su(H) motifs are mutated (H, *Enh3[mut]-GFP*, Green), DAPI (Blue) reveals all nuclei. (**I)** *Notch[NRE]-GFP* (Green) is co-expressed with Zfh1 (Red) in the pMPs associated with the indirect flight muscles; DAPI (Blue) detects all nuclei. (n=12 heminota; from two independent replicates). In G-I anti-P1 was included to label immune cells and exclude them from the analysis. Scale bars: 25 μM.

Figure 5. Expression dynamic of *miR-8* and Zfh1 in MPs and pMPs during indirect flight muscle development. (A-C) *miR-8 (*Green*, miR-8-Gal4>UAS-mCD8::GFP)* is not highly expressed in MPs *(*Cut, Purple) but is prevalent in the wing disc pouch (Arrow), notum (Arrowhead) and air sac (Asterisk). Higher magnification shows that low level of *miR-8* expression can be detected in the subset of MPs where Zfh1 is normally low (Arrowhead in C) but not in other MPs. Scale bars: 50 μM. (n>20 wing discs; from three biological replicates). (**D-D'')** IFM preparation isolated from *miR-8-Gal4>UAS-nlsGFP* pupae at 18-22hr APF. At this stage *miR-8* (Green; D and D') is co-expressed with Zfh1 (Red; D and D'') in MPs but *miR-8* is more highly expressed in differentiated myoblasts (Asterisks in D'), found within the muscles (labeled with Phalloidin, Blue), compared to the undifferentiated MPs, found between the muscles (Arrowheads in D'). In contrast, Zfh1 (D, D") is detected at lower levels in the differentiated myoblasts compared to the undifferentiated MPs (Asterisks in D'). Scale bar: 25μM. **(E-E'')** IFMs preparation isolated

from *miR-8-Gal4 > UAS-nlsGFP* pupae at 30-36hr APF. At this stage, *mir-8* is highly detected in the differentiated muscle nuclei. The majority of the Zfh1+ve pMPs (Red) do not express *mir-8* (Green) (Arrowheads). Few Zfh1+ve pMPs express *mir-8* (Arrows). Scale bar: 50 μM. **(F-F'')** In adult IFMs, *mir-8* (Green) expression is absent from Zfh1+ve (red) pMPs (Arrows, D-D') but is present at uniformly high levels in IFMs, (Phalloidin, Blue). Scale bars: 50μM. (n=20 heminota; from three biological replicates).

Figure 6. The conserved microRNA *miR-8/miR-200* antagonizes *zfh1* to promote muscle differentiation. (A-C) Effect of *miR-8* overexpression (*1151-Gal4 > UAS-miR-8*) on Zfh1 (White) protein level in MPs. Scale Bars: 50 μM. (C) Zfh1 expression is significantly reduced by *miR-8* over-expression. (***p=0.0009, n=12 wing discs in each condition, light and dark shading indicates data points from two independent replicates). **(D-E)** Sagittal sections of adult IFMs stained for Phalloidin (Blue), Zfh1 (Green) and P1 (Red). Down regulating *miR-8* during muscle differentiation (*Mef2-Gal4 > UAS-miR-8-Sp*) increases the final number of adult pMPs. **(F)** The number of pMPs in adult IFMs in the indicated conditions was significantly different. (****$p<0.0001$, n=18 adults for each genotype; light, dark and intermediate shading indicates data points from three independent replicates). Scale bars: 100 μM.

Figure 6-figure supplement 1. *miR-8* responds to high level of Mef2. *miR-8* activity was detected using *miR-8-EGFP* sensor (Kennel et al., 2012). **(A-B)** Effect of Mef2 overexpression (*1151-Gal4>UAS-Mef2*) on *miR-8* sensor (Green) expression level in MPs. *miR-8* sensor expression in MPs is significantly reduced by Mef2 overexpression (Arrows in A' and B'). Zfh1 expression (Red) was used to visualize the MPs. **(C)** Quantification of *miR-8* Sensor intensity in the indicated conditions. (**p<0.01, n=12 wing discs for each indicated genotype). In each condition light and dark shading indicates data points from two independent replicates. Scale bars=50 μM. **(D)** Prolonged *miR-8* overexpression in the adult pMPs (*Enh3-Gal4; Gal80ts*>UAS-*miR-8*) significantly affects the muscle homeostasis. (****p<0.0001, n=16 for each genotype). In each condition light, dark and intermediate shading indicates data points from three independent replicates.

Figure 7. (A) Schematic representation of *zfh1* isoforms. *zfh1-short* (*zfh1-RA*) is initiated from a different transcription start site and has shorter 3'UTR that lacks the target site for *miR-8* (Green; (Antonello, et al., 2015)) present in *zfh1-long* isoforms (*zfh1-RB, zfh1-RE*); the position of the *miR-8* seed sites in *zfh1-long* 3' UTR are depicted. Non-coding exons

and coding exons are depicted by grey and black boxes respectively, red lines indicate the probes used for FISH experiments in B-E. **(B-C)** *zfh1-long* is present uniformly in MPs. (n>10 wing discs from two replicates; B, Green and B', White) whereas *zfh1-short* is only detected in a few MPs (n>15 wing discs from three replicates; C, Green and C', White), detected by *in situ hybridisation* in wild type third instar wing discs stained for Zfh1 (Purple). Scale bars: 10μM. (B" B"', C" C"') Higher magnifications of boxed regions (Scale bars: 50 μM). **(D-E)** In adult IFMs *zfh1-long* is detected in the pMPs (n=11 pMPs from two replicates, arrow in D') and in some differentiated nuclei located in their vicinity (arrowheads in D') whereas *zfh1-short* is only present in pMPs (n=15 pMPs from two replicates, arrow in E'). *Enh3* expression (Green, *Enh3-Gal4>UAS-mCD8GFP*) labels adult pMPs and Mef2 (Blue) labels all muscle nuclei**.** Scale bars: 20μM**.**

Figure 7-figure supplement 1. (A) Domain structure of Drosophila Zfh1 protein isoforms E, B and A. Purple bars indicate the predicted zinc fingers, Green bar indicates the predicted homeodomain. All three protein-isoforms contain the core zinc finger and homeodomains needed for Zfh1 DNA-binding activity. Isoforms E and B contain two additional N-terminal zinc fingers (Postigo, et al., 1999). **(B-H)** Zfh1-short protects the MPs from differentiation. B. Overexpression of Mef2 in the MPs (*1151-Gal4>Mef2; white-RNAi*) induces premature muscle differentiation revealed by the ectopic expression of the *MHC-lacZ* reporter (Purple). This phenotype is associated with reduced MPs (β3-Tub, Green). **(C)** Co-expression of Mef2 along with Zfh1-Short (*1151-Gal4>Mef2; Zfh1-Short*) rescues the premature differentiation phenotype. **(D-E)** Quantification of the differentiation area (D) and the progenitor area (I) in the indicated genotypes. (D, p=0.0025 and E, p=0.0002. n=12 wing discs ; from two biological replicates).

Figure 8. *zfh1-short* regulation by Notch is important to maintain muscle homeostasis. (A-C) Expression of an activated Notch (*1151-Gal4>UAS-NΔECD*) in MPs induces ectopic *zfh1-short* transcription. *In situ* hybridisation detecting *zfh1-short* (Green) in MPs (Zfh1, Purple) with wild type (A-A') or elevated Notch activity (B-B'). Scale bars: 50 μM. **(C)** Quantification showing significant increase in *zfh1-short* transcriptional dots upon Notch up regulation, relative to total number of MPs (**p< 0.01, Student t-test; n=14 wing discs for each genotype, light and dark shading indicates data points from two independent replicates). **(D-H)** Notch depletion leads to a severe decrease in *zfh1-short* (Red) (E'-F' and D) in pMPs (Green; *Enh3-Gal4; UAS-mCD8GFP >UAS-Notch-RNAi; tubGal80ts*) and to an increase in Mef2 levels (Blue) (E-F' and H). **(G-G' and H)** *zfh1*

depletion in the pMPs (*Enh3-Gal4; UAS-mCD8GFP >UASzfh1RNAi; tubGal80ts*) leads to an increase in Mef2 levels (Blue). Scale bars: 25 μM. Quantifications of *zfh1-short* (D) and Mef2 (H) in the indicated conditions show that the levels are significantly different (D, n=21 pMPs for each genotype (***p*<0.01); H, n=15 pMPs for Control *RNAi* and n=13 pMPs for *Notch RNAi* (**p*<0.05) and n=14 pMPs for *Zfh1 RNAi* (***p*<0.01)). In each condition light, dark and intermediate shading indicates data points from three independent replicates. **(I)**. Prolonged *Notch* depletion in the pMPs (*Enh3-Gal4; Gal80ts > UAS-Notch RNAi*) affects the muscle homeostasis. (***p*<0.01, n=14 for each genotype, light and dark shading indicates data points from two independent replicates).

Figure 8-figure supplement 1. Notch activity is not necessary for *zfh1-long* (Red) transcription (A'-B' and C) in pMPs (Green; *Enh3-Gal4; UAS-mCD8GFP > white-RNAi*). *Enh3-Gal4* was used to drive expression of control RNAi (A-A'), *Notch* RNAi (B,B') specifically in pMPs (*Enh3-Gal4; UAS-mCD8GFP > UAS-Notch RNAi; tubGal80ts)*. Mef2 (Blue) marks all muscle and pMPs nuclei. Scale bars: 25μM. **(C)** Quantification of *zfh1-long* intensity in the indicated conditions. *zfh1-long* transcriptional intensity measured from control RNAi and *Notch RNAi* were not statistically different (ns) (*p*=0.8190, n=15 (control *RNAi*) and n=14 (*Notch RNAi*)). *zfh1-long* transcriptional intensity quantifications were generated from two independent replicates, indicated by light and dark shading.

Figure 9. Model summarizing the role of alternate *zfh1* isoforms in the maintenance of adult pMPs. *zfh1-long* (Grey) is expressed in all MPs at larval stage. Silencing of *zfh1-long* by *miR-8* (Red) facilitates the MPs differentiation. *zfh1-short* (Green) transcription is driven and maintained in pMPs by a Notch responsive element (Enh3, Green rectangle), which may also contribute to *zfh1-long* regulation. Because *zfh1-short* is insensitive to *miR-8*, Zfh1 protein is maintained in pMPs, enabling them to escape differentiation and persist as MPs in the adult.

Figure 1

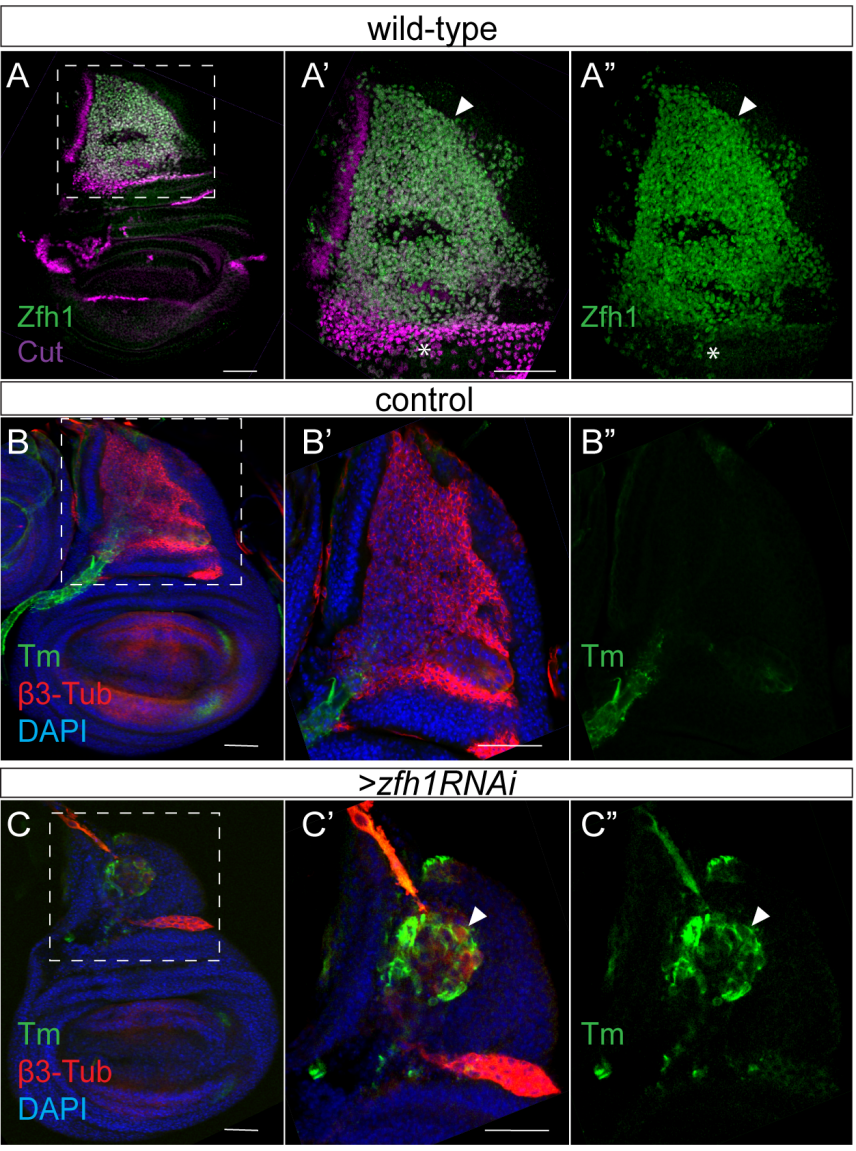
wild-type
A
Zfh1
Cut
A'
A"
Zfh1
control
B
Tm
β3-Tub
DAPI
B'
B"
Tm
>zfh1RNAi
C
Tm
β3-Tub
DAPI
C'
C"
Tm

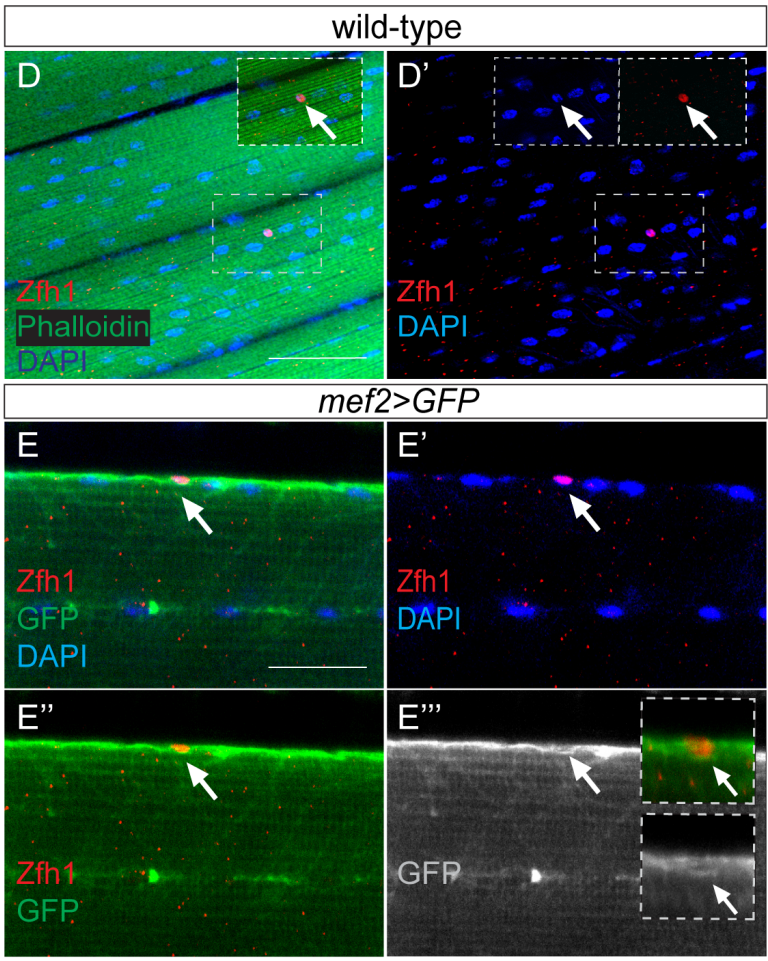
wild-type
D
Zfh1
Phalloidin
DAPI
D'
Zfh1
DAPI
mef2>GFP
E
Zfh1
GFP
DAPI
E'
Zfh1
DAPI
E"
Zfh1
GFP
E'"
GFP

Figure 2

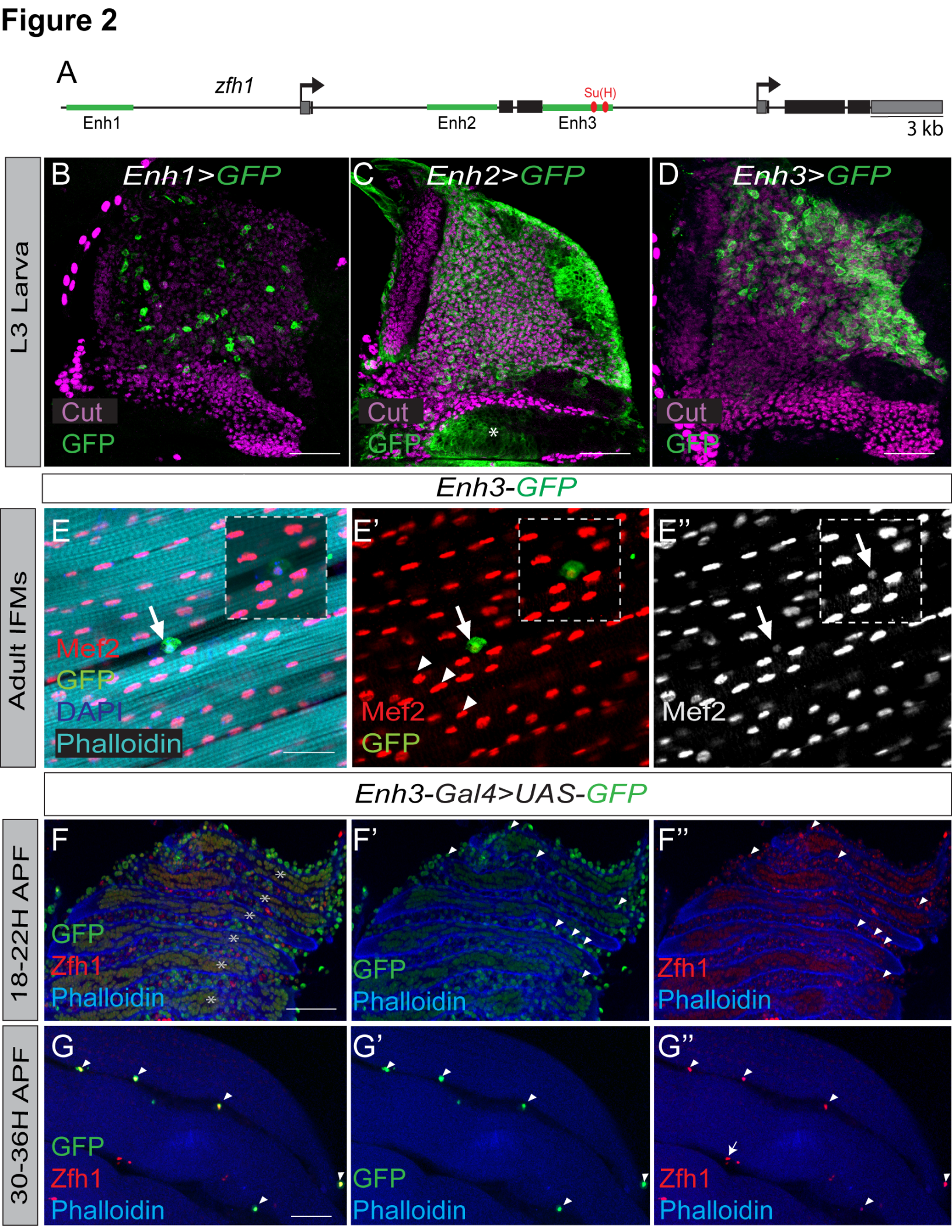
A
zfh1
Su(H)
Enh1
Enh2
Enh3
3 kb
L3 Larva
B Enh1>GFP
C Enh2>GFP
D Enh3>GFP
Cut
GFP
Enh3-GFP
Adult IFMs
E
E'
E''
Mef2
GFP
DAPI
Phalloidin
Enh3-Gal4>UAS-GFP
18-22H APF
F
F'
F''
Zfh1
30-36H APF
G
G'
G''

Figure 3

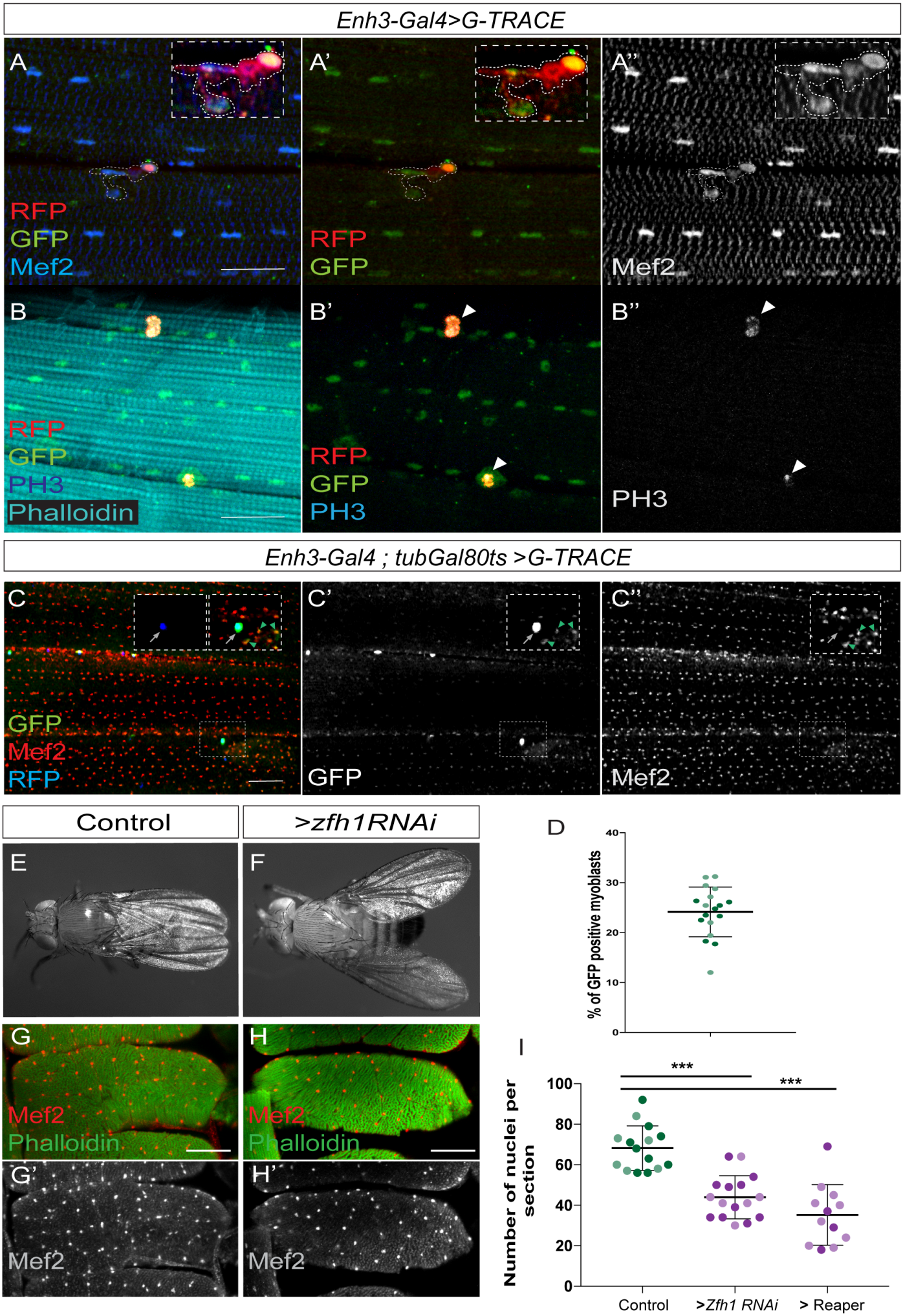
Enh3-Gal4>G-TRACE
A
RFP
GFP
Mef2
A'
RFP
GFP
A''
Mef2
B
RFP
GFP
PH3
Phalloidin
B'
RFP
GFP
PH3
B''
PH3
Enh3-Gal4 ; tubGal80ts >G-TRACE
C
GFP
Mef2
RFP
C'
GFP
C''
Mef2
Control
>zfh1RNAi
E
F
G
Mef2
Phalloidin
H
Mef2
Phalloidin
G'
Mef2
H'
Mef2
D
% of GFP positive myoblasts
40
30
20
10
0
I
Number of nuclei per section
***
***
100
80
60
40
20
0
Control
>Zfh1 RNAi
> Reaper

Figure 4.

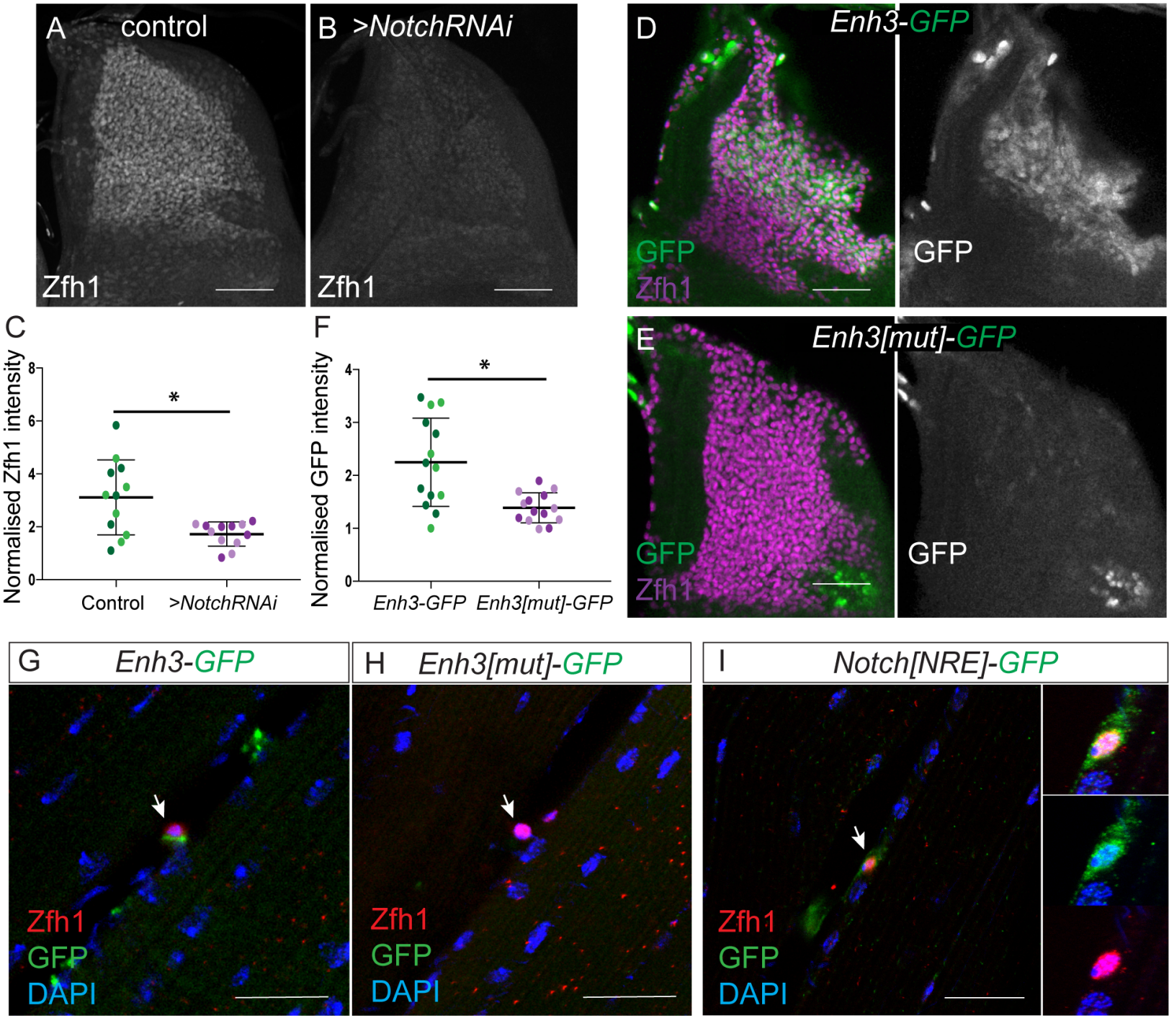
A control
Zfh1
B >NotchRNAi
Zfh1
C
Normalised Zfh1 intensity
Control
>NotchRNAi
D Enh3-GFP
GFP
Zfh1
GFP
E Enh3[mut]-GFP
GFP
Zfh1
GFP
F
Normalised GFP intensity
Enh3-GFP
Enh3[mut]-GFP
G Enh3-GFP
Zfh1
GFP
DAPI
H Enh3[mut]-GFP
Zfh1
GFP
DAPI
I Notch[NRE]-GFP
Zfh1
GFP
DAPI

Figure 5

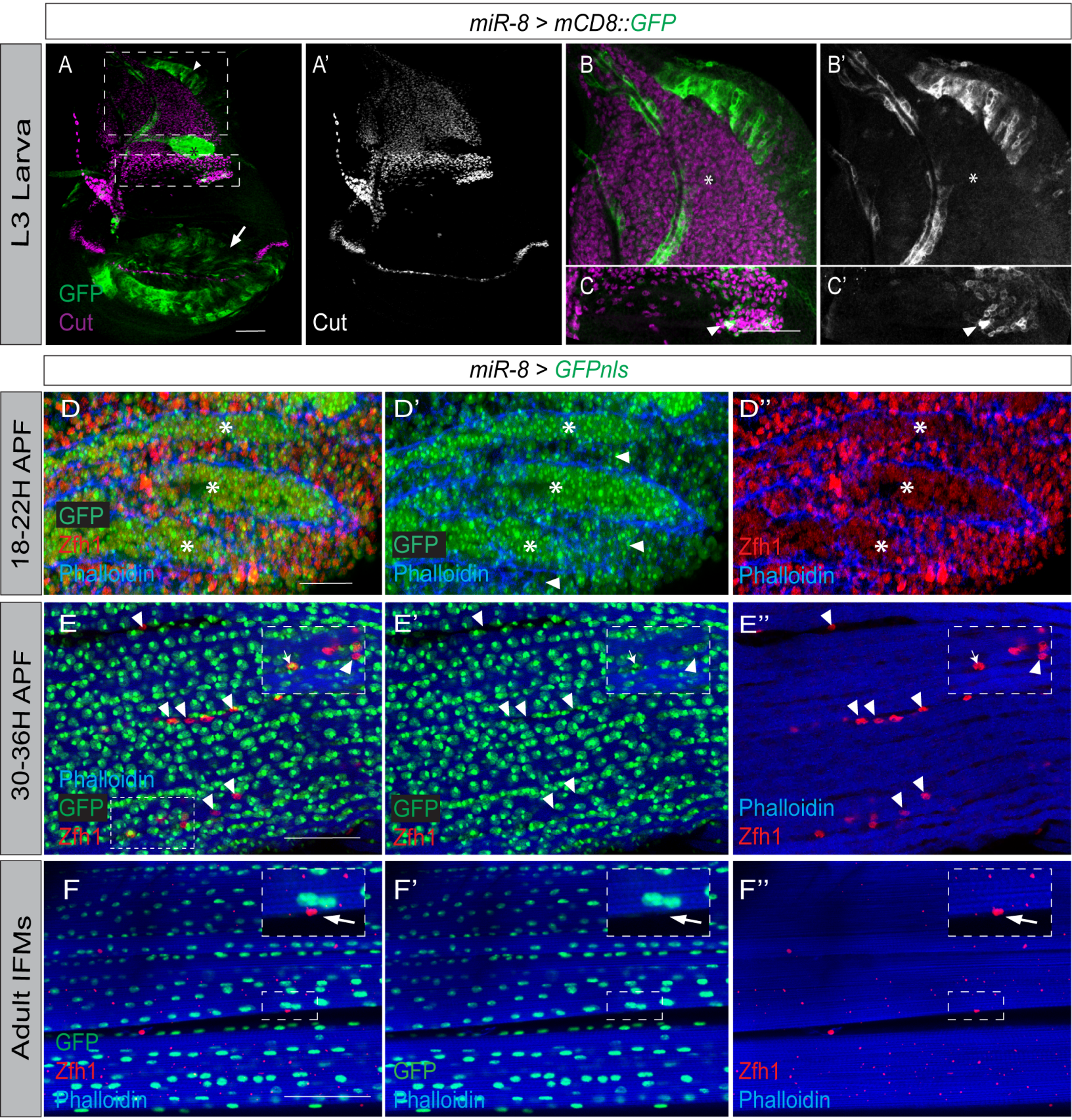
miR-8 > mCD8::GFP
L3 Larva
A
A'
B
B'
C
C'
GFP
Cut
Cut
miR-8 > GFPnls
18-22H APF
D
D'
D''
GFP
Zfh1
Phalloidin
GFP
Phalloidin
Zfh1
Phalloidin
30-36H APF
E
E'
E''
Phalloidin
GFP
Zfh1
GFP
Zfh1
Phalloidin
Zfh1
Adult IFMs
F
F'
F''
GFP
Zfh1
Phalloidin
GFP
Phalloidin
Zfh1
Phalloidin

Figure 6

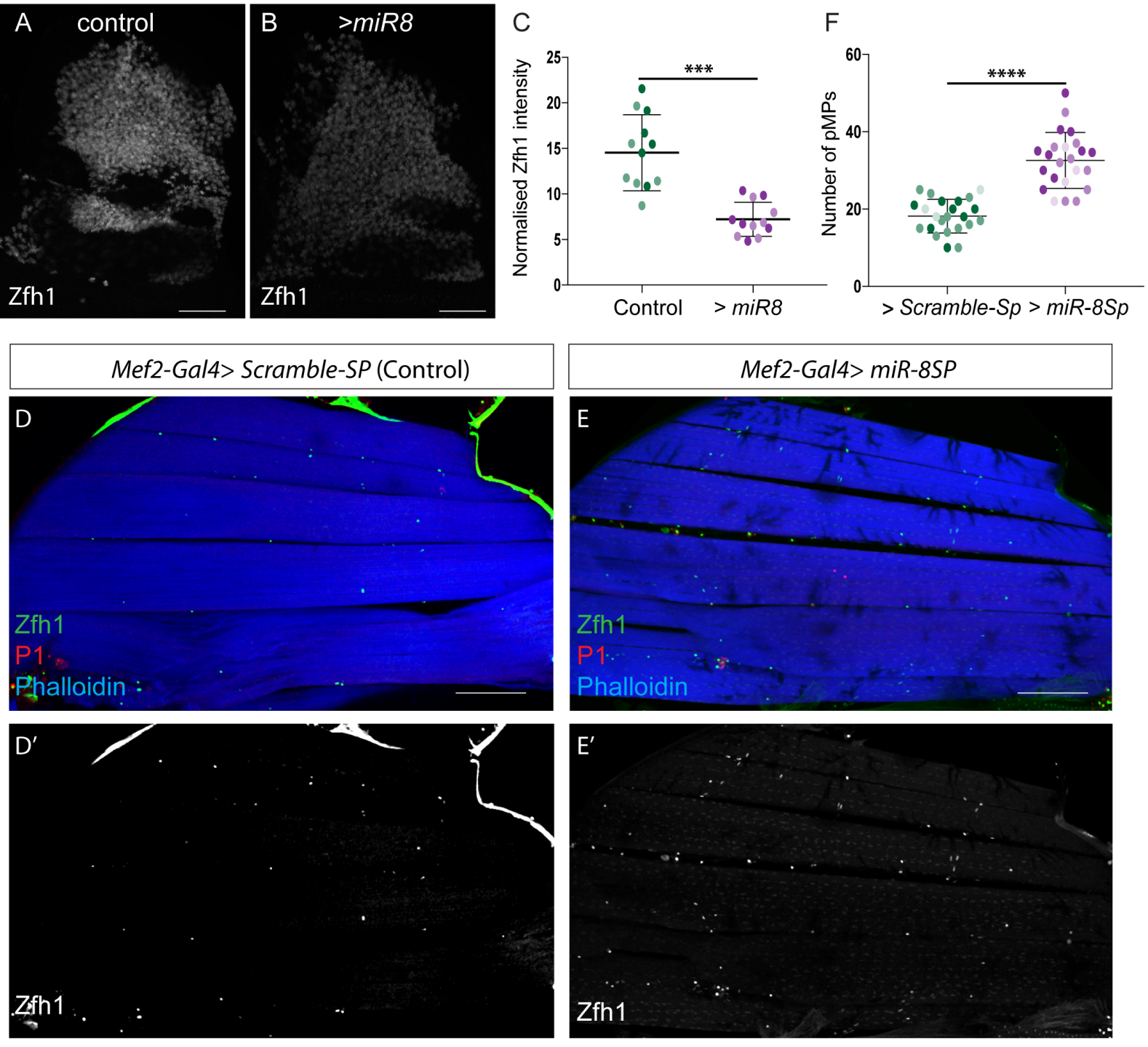
A control
Zfh1
B >miR8
Zfh1
C
Normalised Zfh1 intensity
***
Control
> miR8
F
Number of pMPs
****
> Scramble-Sp
> miR-8Sp
Mef2-Gal4> Scramble-SP (Control)
Mef2-Gal4> miR-8SP
D
Zfh1
P1
Phalloidin
E
Zfh1
P1
Phalloidin
D′
Zfh1
E′
Zfh1

Figure 7

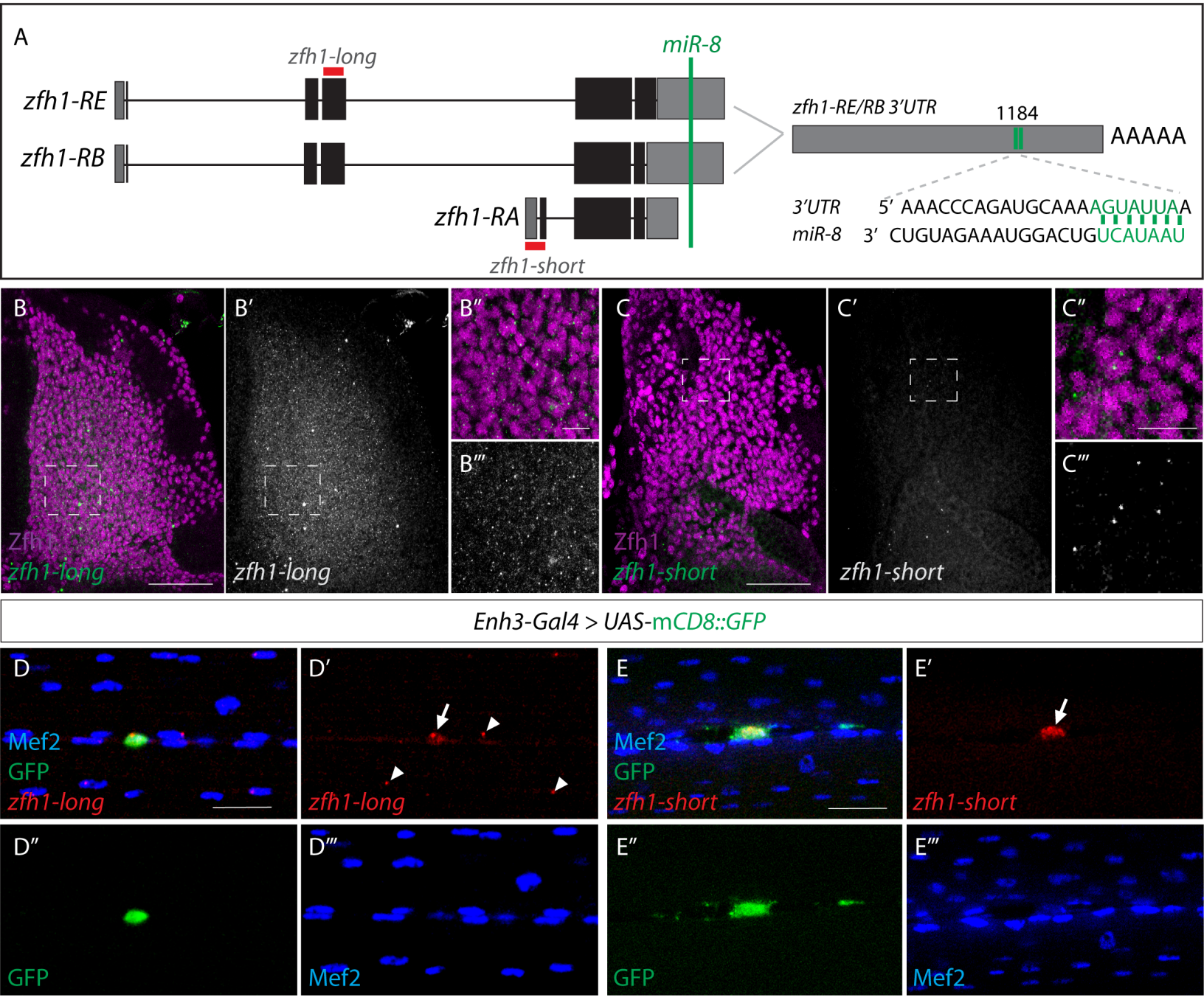
A
zfh1-long
miR-8
zfh1-RE
zfh1-RB
zfh1-RA
zfh1-short
zfh1-RE/RB 3'UTR
1184
AAAAA
3'UTR 5' AAACCCAGAUGCAAAAGUAUUAA
miR-8 3' CUGUAGAAAUGGACUGUCAUAAU
B
B'
B''
B'''
C
C'
C''
C'''
Zfh1
zfh1-long
zfh1-long
Zfh1
zfh1-short
zfh1-short
Enh3-Gal4 > UAS-mCD8::GFP
D
D'
D''
D'''
E
E'
E''
E'''
Mef2
GFP
zfh1-long
zfh1-long
GFP
Mef2
Mef2
GFP
zfh1-short
zfh1-short
GFP
Mef2

Figure 8

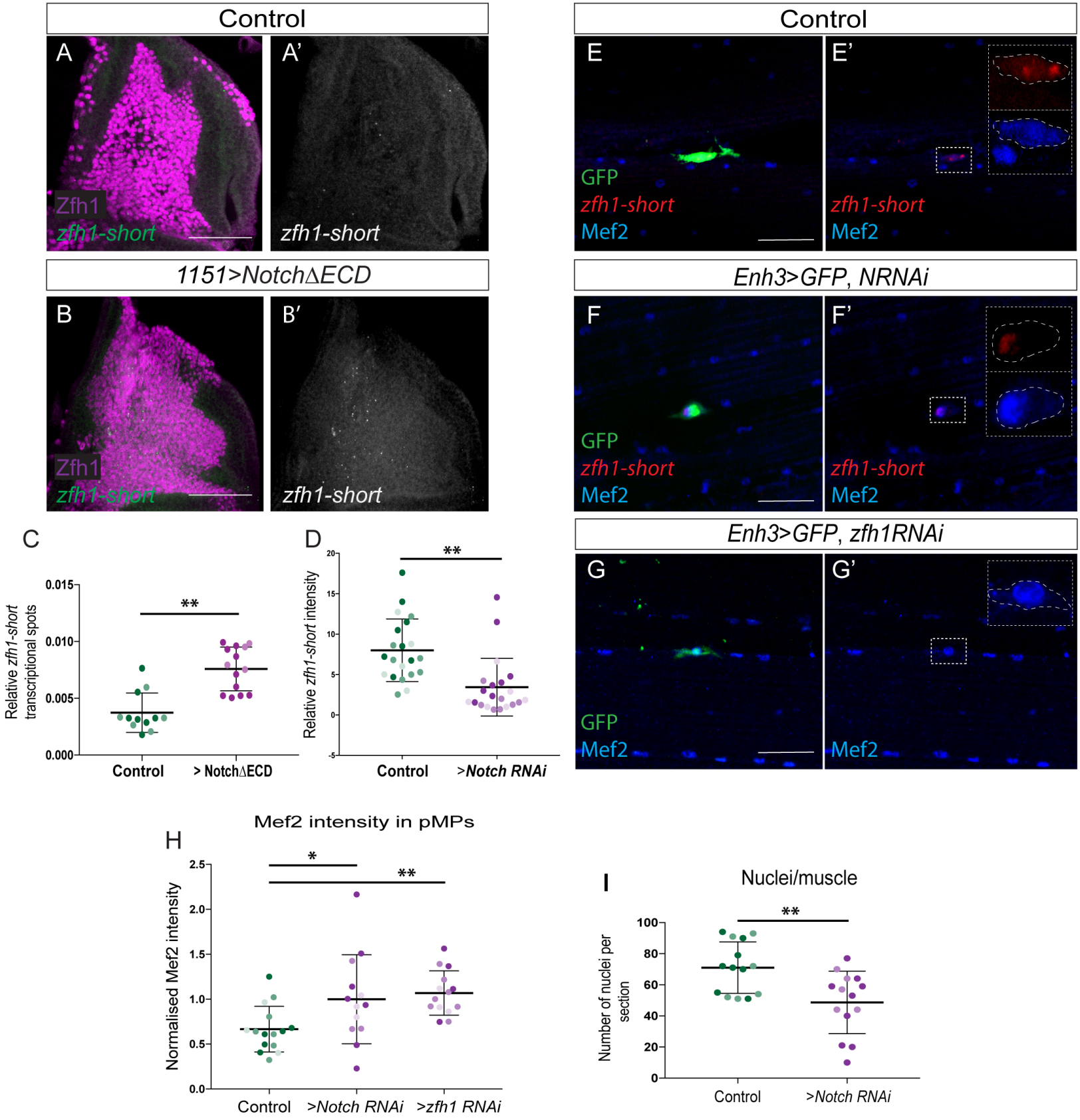
Control
A
A'
Zfh1
zfh1-short
zfh1-short
1151>NotchΔECD
B
B'
Zfh1
zfh1-short
zfh1-short
Control
E
E'
GFP
zfh1-short
Mef2
zfh1-short
Mef2
Enh3>GFP, NRNAi
F
F'
GFP
zfh1-short
Mef2
zfh1-short
Mef2
Enh3>GFP, zfh1RNAi
G
G'
GFP
Mef2
Mef2
C
Relative zfh1-short transcriptional spots
0.015
0.010
0.005
0.000
**
Control
> NotchΔECD
D
Relative zfh1-short intensity
20
15
10
5
0
-5
**
Control
>Notch RNAi
H
Mef2 intensity in pMPs
Normalised Mef2 intensity
2.5
2.0
1.5
1.0
0.5
0.0
*
**
Control
>Notch RNAi
>zfh1 RNAi
I
Nuclei/muscle
Number of nuclei per section
100
80
60
40
20
0
**
Control
>Notch RNAi

Figure 9

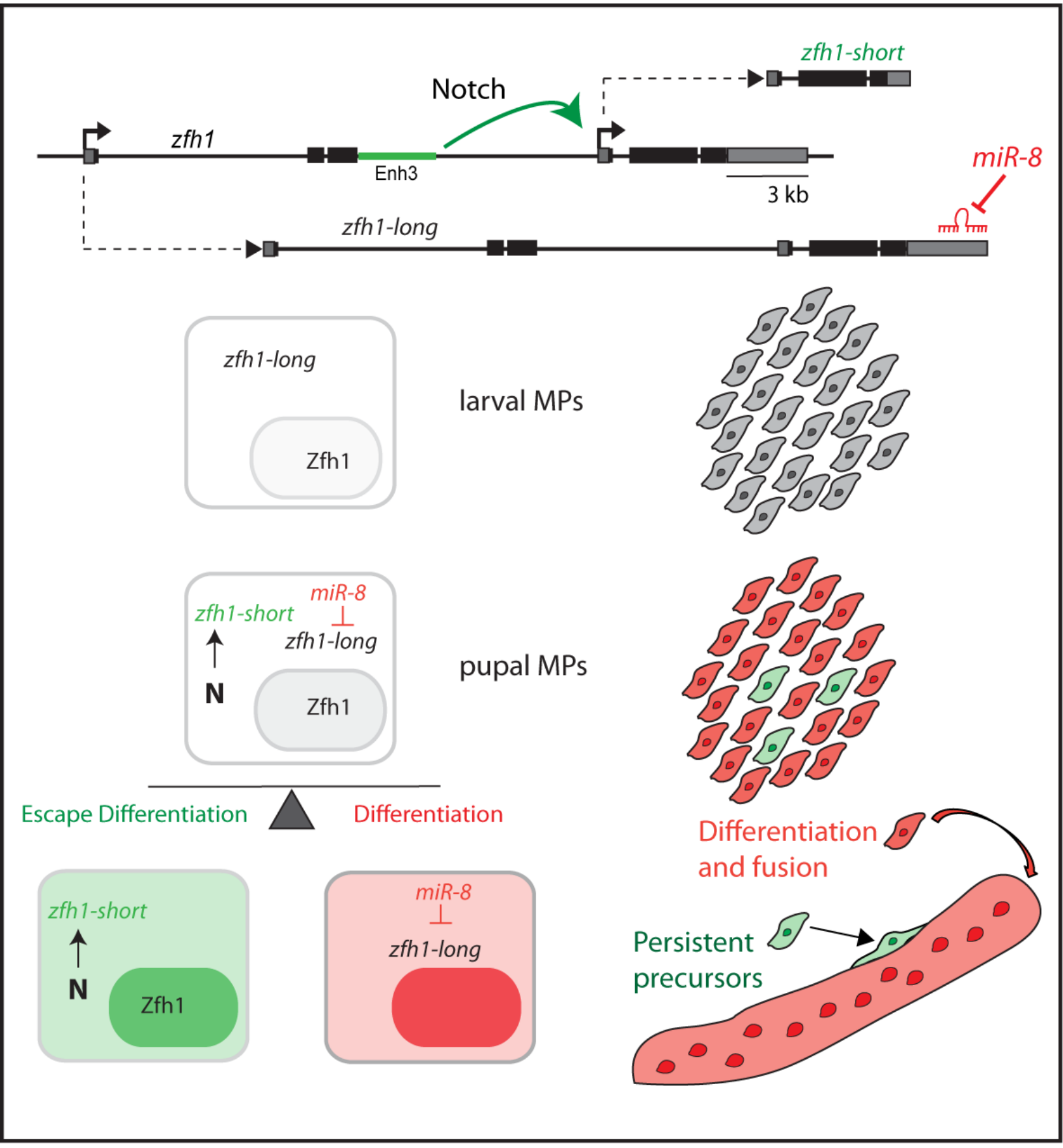
zfh1-short
Notch
zfh1
Enh3
3 kb
miR-8
zfh1-long
zfh1-long
Zfh1
larval MPs
miR-8
zfh1-short
zfh1-long
N
Zfh1
pupal MPs
Escape Differentiation
Differentiation
Differentiation and fusion
zfh1-short
N
Zfh1
miR-8
zfh1-long
Persistent precursors

Figure supplement 1

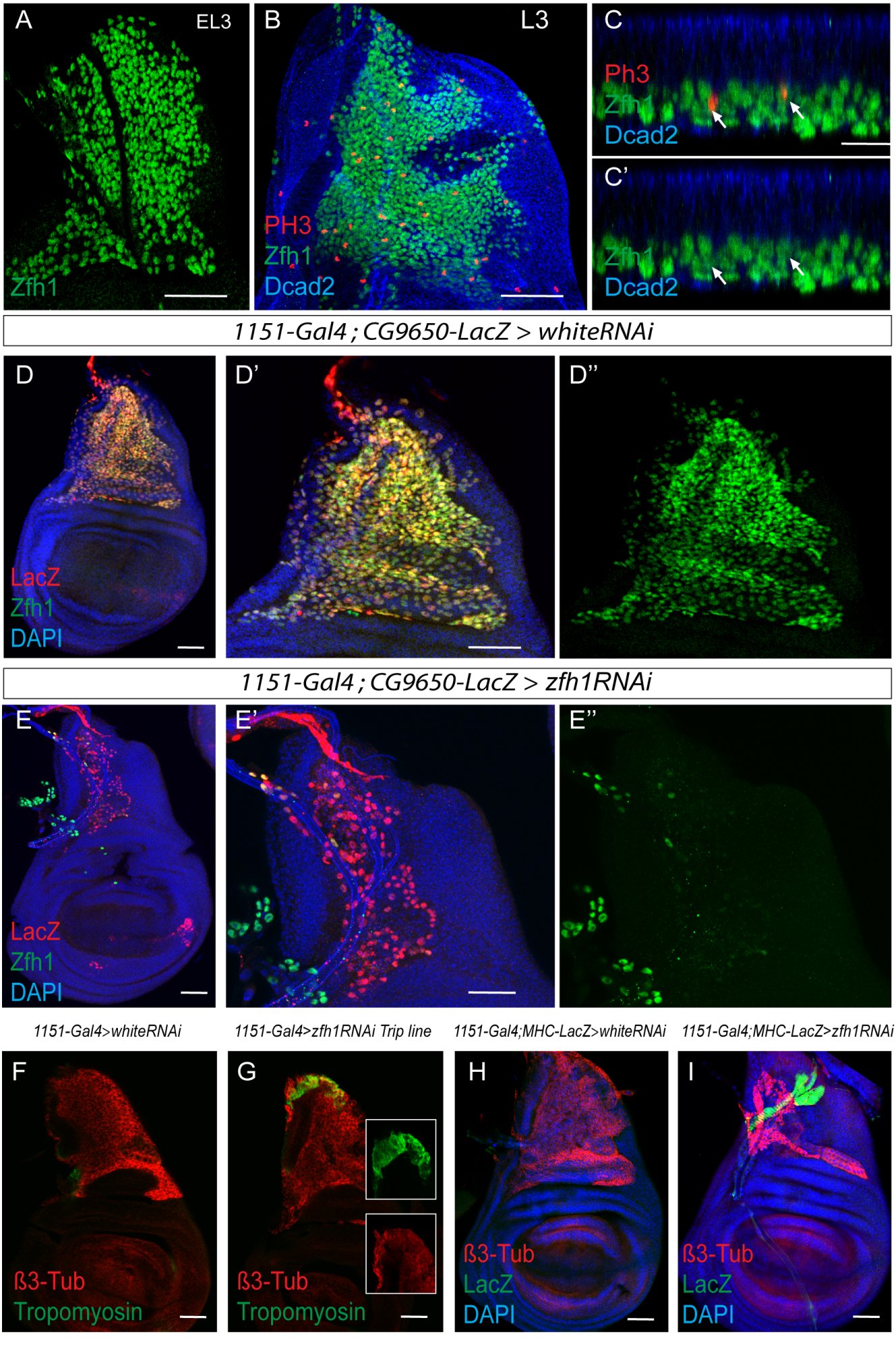

Figure supplement 2

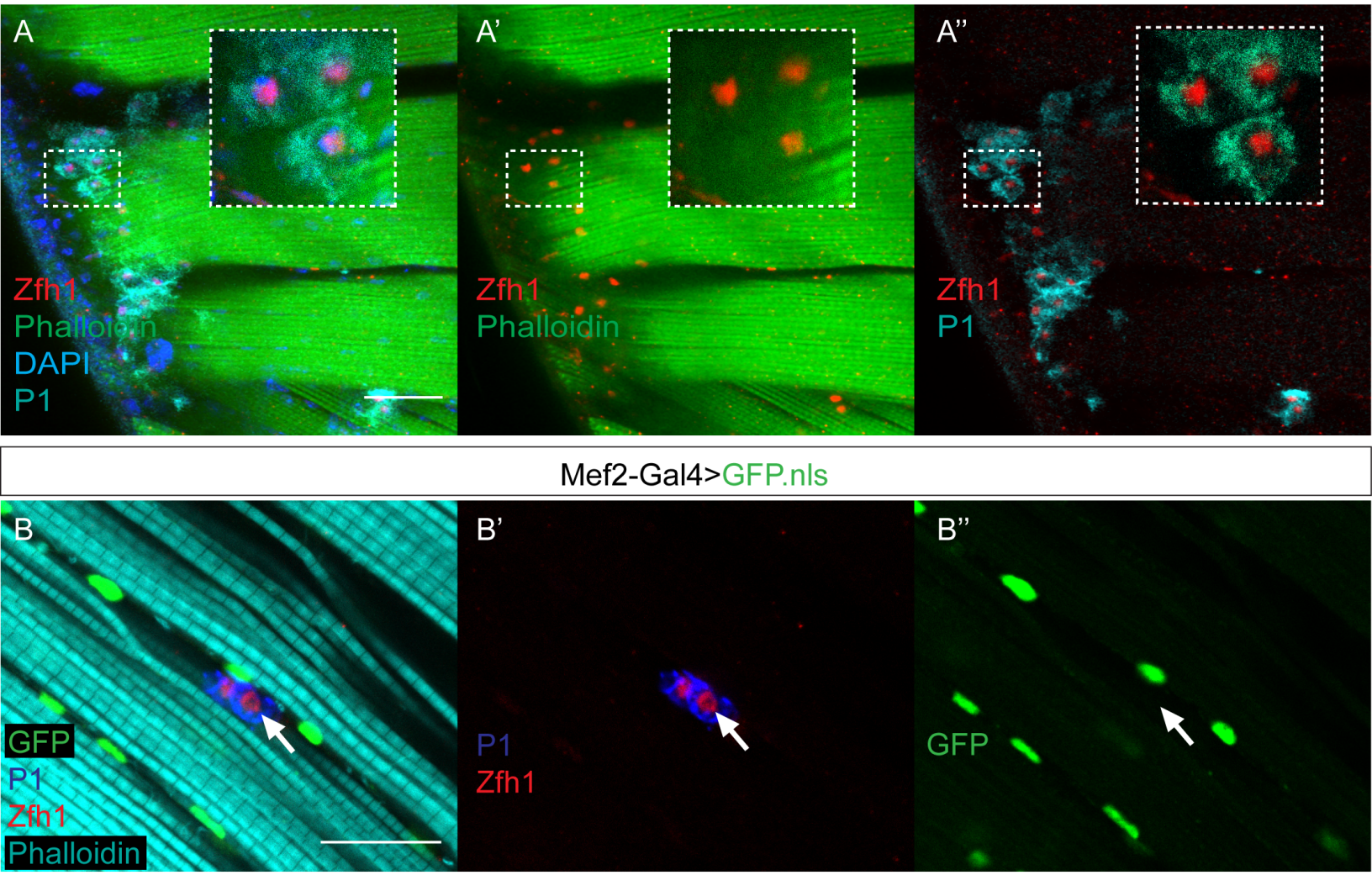

Figure supplement 3

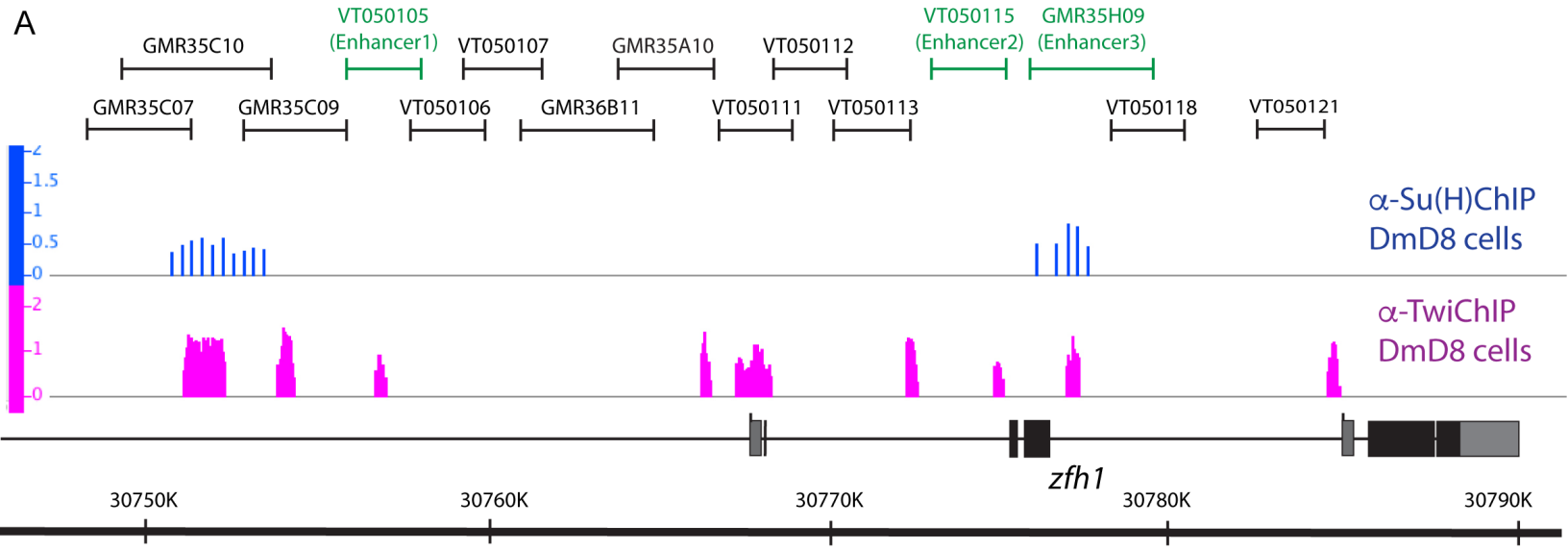

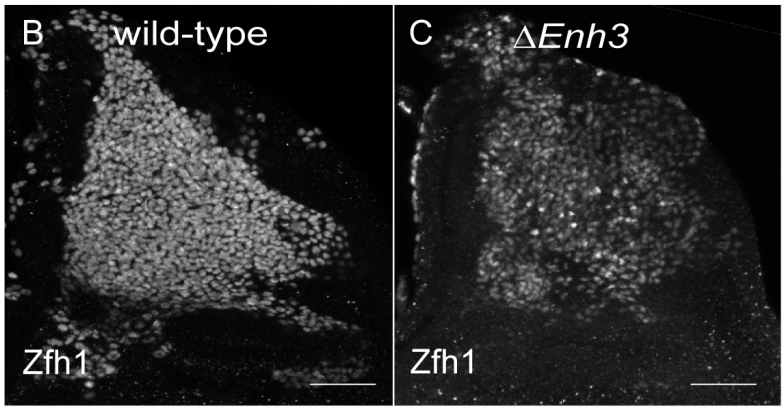

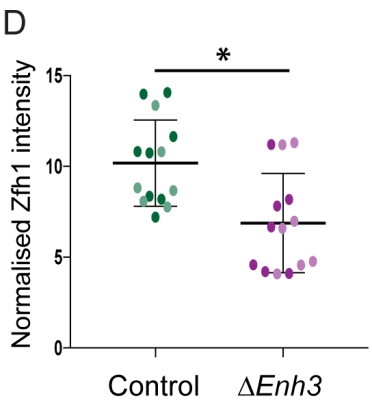

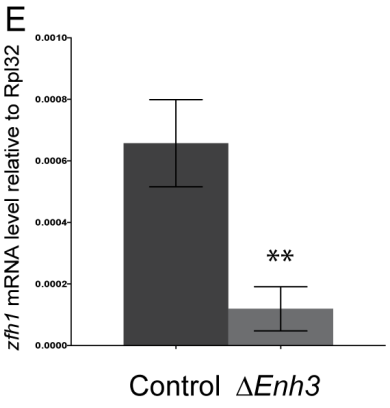

Figure supplement 4

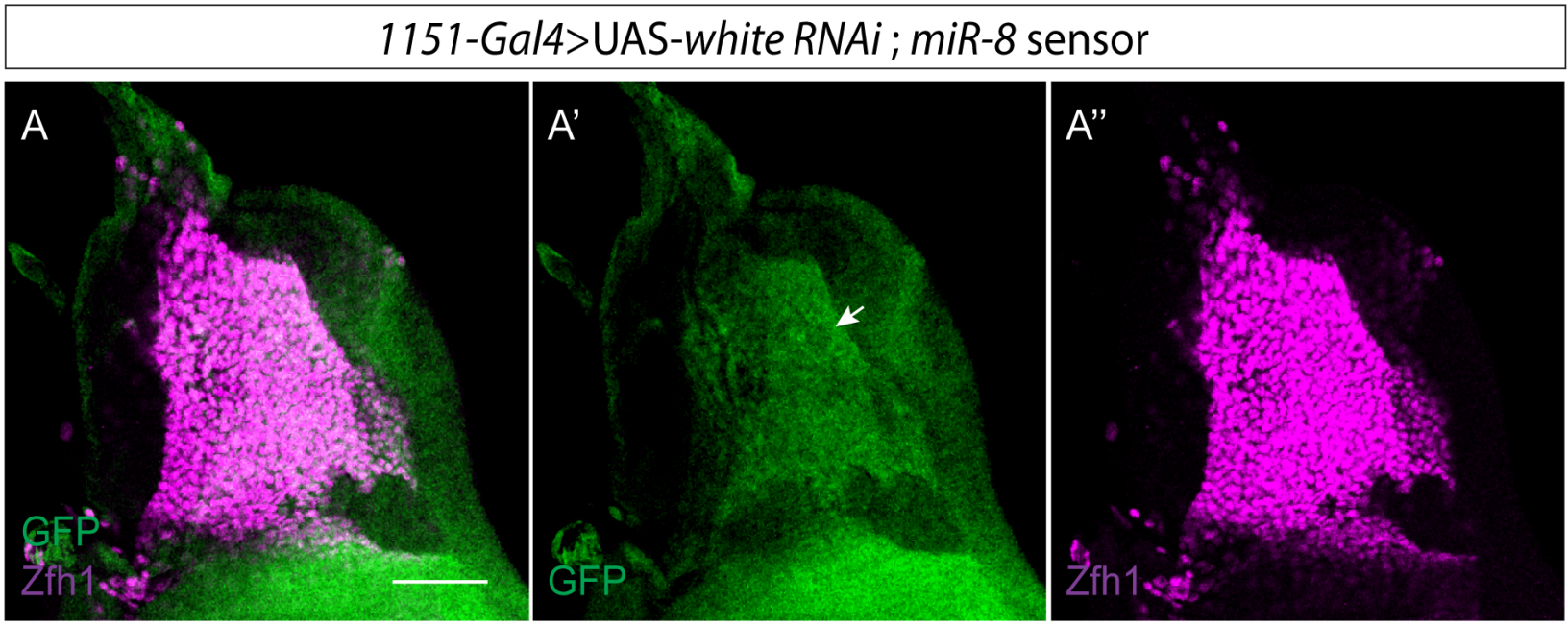

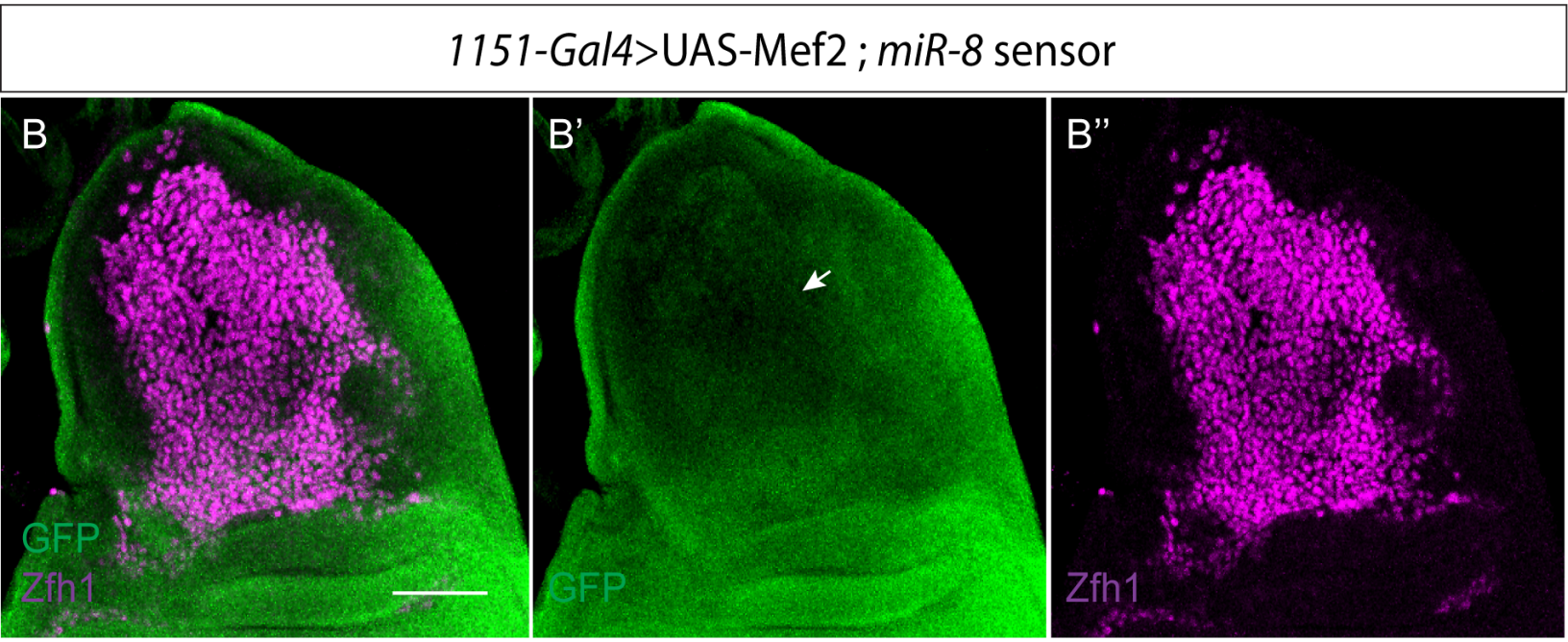

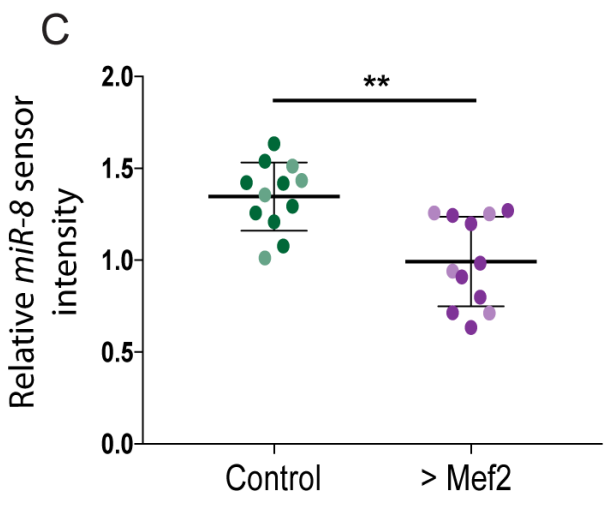

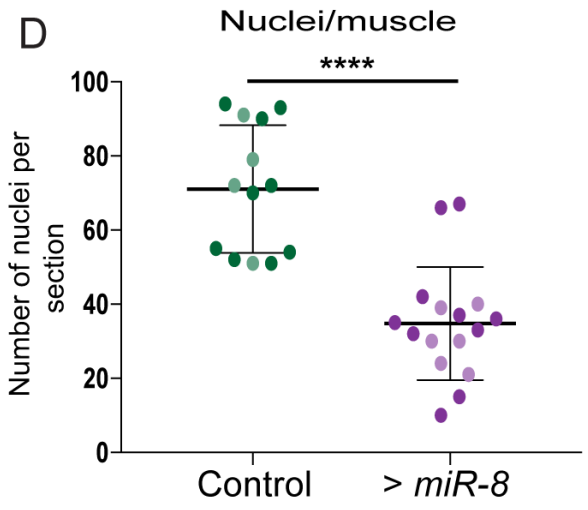

Figure supplement 5

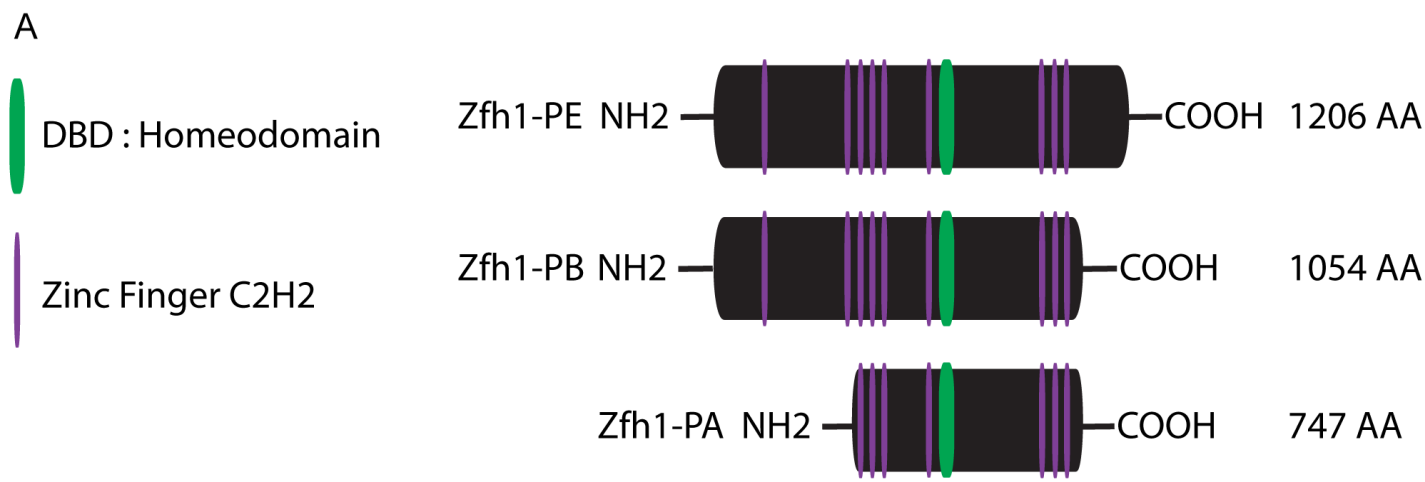

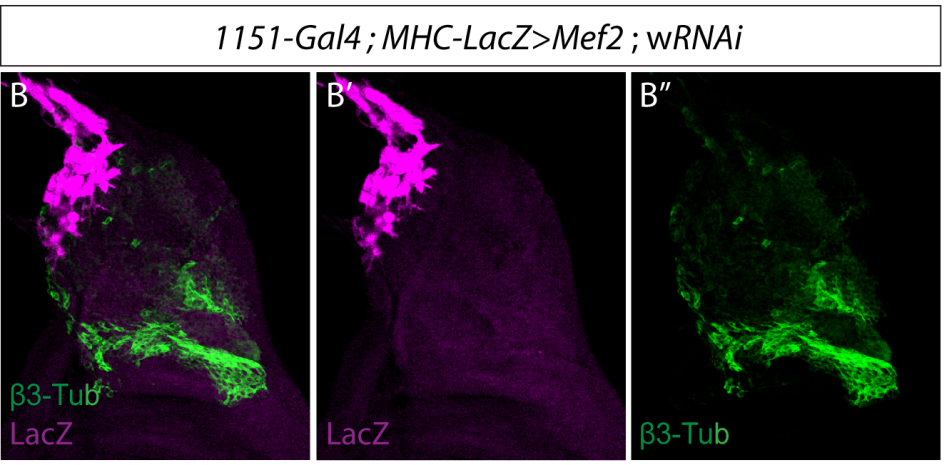

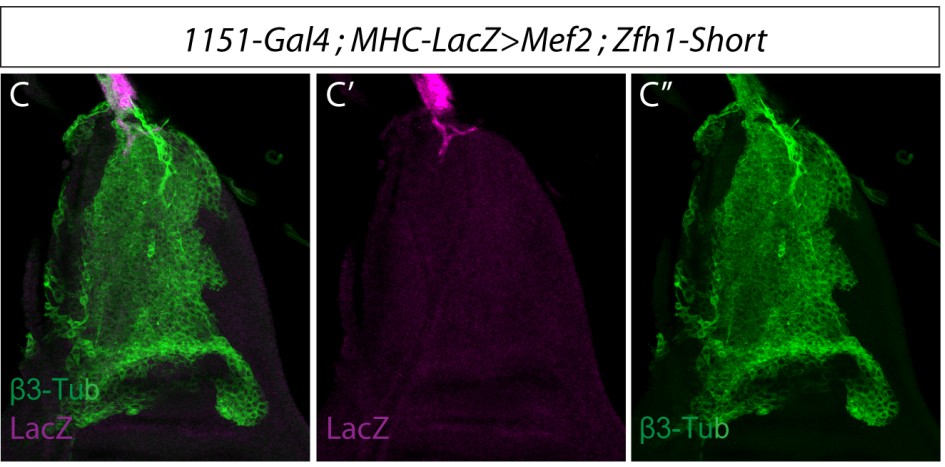

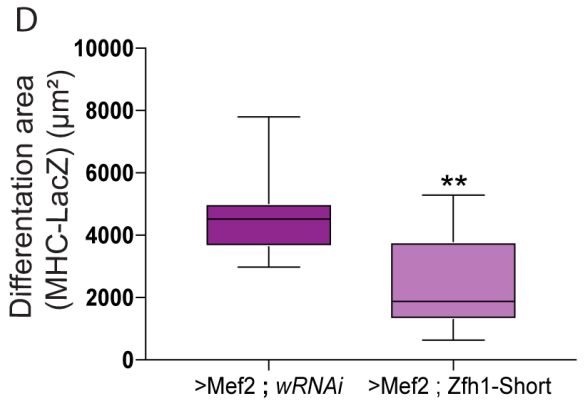

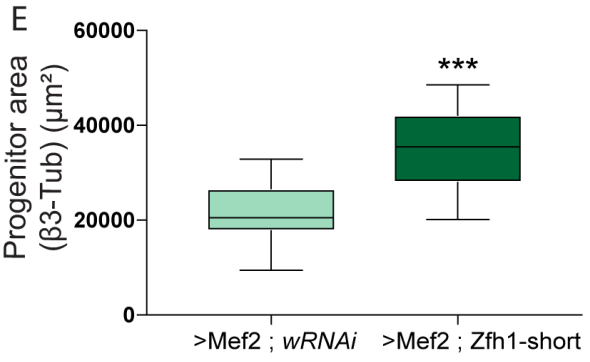

Figure supplement 6